TR 64-304.5

INVESTIGATION OF ELECTRO-OPTIC TECHNIQUES FOR CONTROLLING THE DIRECTION OF A LASER BEAM

V. J. Fowler

Final Report

Contract NASw-731

National Aeronautics and Space Administration

George C. Marshall Space Flight Center

Huntsville, Alabama

Issued: 10 August 1964

GENERAL TELEPHONE & ELECTRONICS LABORATORIES

INCORPORATED

BAYSIDE LABORATORIES, BAYSIDE, NEW YORK

TR 64-304.5

INVESTIGATION OF ELECTRO-OPTIC TECHNIQUES FOR CONTROLLING THE DIRECTION OF A LASER BEAM

V. J. Fowler

Final Report

Contract NASw-731

National Aeronautics and Space Administration
George C. Marshall Space Flight Center
Huntsville, Alabama

Issued: 10 August 1964

General Telephone & Electronics Laboratories Inc.
Bayside, New York

ABSTRACT

28886

An investigation of electro-optic and piezoelectric methods for precision rapid deflection of laser beams is described. The program included the design, development, and evaluation of a number of electro-optic variable refraction deflectors and piezoelectric shear-plate mirror deflectors. These structures all have inherent capabilities for extremely rapid deflection, although high-speed operation was not an objective of this program. It was determined that these structures could be designed to achieve deflection angles of about one degree with minimum beam angles of about 0.01 degree. Relatively large amounts of stored energy are required to obtain maximum deflection, necessitating the use of narrow-band deflection signals for operation at scan frequencies in the range from 10 to 100 kc/s. Precision deflection is feasible but difficult, requiring temperature stabilization and high field correction.

Author

TABLE OF CONTENTS

TABLE OF CONTENTS (cont'd.)

1. INTRODUCTION

Laser beams have been under investigation for possible use in aerospace communications for a number of reasons. The main advantage sought from coherent light is the very great directivity that can be obtained with radiating structures of modest size. Antenna gains in excess of 120 dB appear to be feasible for optical lenses and mirrors of less than a foot diameter, whereas less than 30 dB can be obtained in microwave antennas of comparable size. Although part of the increased gain of an optical antenna may be needed to offset a smaller receiver sensitivity, it appears that optical communication systems should be able to achieve much longer ranges with much larger information bandwidths than radio or microwave systems of comparable transmitter power and antenna size.

Application of these much narrower beam widths calls for significant advances in the art of automatic signal tracking. Present mechanical means for steering microwave antennas apparently cannot be extended to meet this need. Instead, it will be necessary to incorporate some means of inertialess electrical steering to obtain adequate precision and speed of operation.

The objective of this program was to devise and test electro-optic methods for rapid light-beam scanning applicable in automatic tracking of extremely narrow laser beams for various applications of interest to NASA. For purposes of comparison, high-speed electrically controlled mirrors were also investigated in this program. Specific goals for this first-year effort were to analyze, design, construct, and evaluate device models with intrinsic capabilities for high-speed operation. The models were to be designed to achieve one-dimensional scanning over maximum angles of about one degree with apertures large enough to accommodate laser beams having diffraction-limited half-intensity beam widths of about 0.01 degree.

The work performed in this program consisted of theoretical studies, deflector model development, and testing of these models at low frequencies to determine their capabilities and limitations for precision deflection. The tests were limited to frequencies well below the lowest acoustic resonant frequencies of the models. This work is being extended under Contract NAS8-11459 with a principal emphasis on models operating at and near acoustic resonance in the range from 10 to 100 kc/s.

2. METHODS FOR RAPID LASER BEAM SCANNING

There are a number of ways in which rapid, electrically controlled laser beam deflection can be accomplished. The ones that we have considered at the GT&E Laboratories can be grouped in three categories: (1) variable refractors, (2) variable reflectors, and (3) variable diffractors. Although each of these is discussed in the following sections, this program was mainly concerned with variable refractors utilizing the Pockel's electro-optic effect in solids.

2.1 VARIABLE-REFRACTION DEFLECTORS

Variable-refraction deflectors utilize electrically controllable refractive media to produce changes in the angle of refraction of light. The operation of these devices is based on the fact that the angle of refraction of a light beam passing through a dense refractive medium, such as a transparent crystal, plastic, or glass, is a function of the index of refraction n of that medium, and therefore this angle can be controlled by controlling n. Various methods can be used to produce small changes in n, including the Pockels and Kerr electro-optic effects, the Brewster elasto-optic (or photoelastic) effect, and the Cotton-Mouton magneto-optic effect. With the electro-optic effects, electric fields are applied to the refractive medium to produce changes in n. Similarly, magnetic fields from electromagnets or solenoids are applied to magneto-optic materials. Use of the elasto-optic effect requires conversion of electric energy to mechanical energy, which can be accomplished in various ways, including the use of piezoelectric or electrostrictive crystals or ceramics, or magnetostrictive metals or ferrites. Electro-dynamic units, such as are used in loudspeakers, could also be used. An elasto-optic variable-refraction deflector would then consist of two parts: an elasto-optic element and an electro-mechanical transducer element.

Deflection devices made with refractors using the Pockels electro-optic effect appear to be the most promising for high-frequency applications. They can be made simple, light, and compact. Refractors using the elasto-optic effect have also received considerable attention because much larger changes of n can be produced in the best elasto-optic materials than in present electro-optic materials. Magneto-optic refractors are not very promising because the maximum change in refractive index is much smaller in magneto-optic materials than in electro-optic materials, and it is much more difficult to produce strong magnetic fields at high frequencies than it is to produce strong electric fields.

Variable refractors can be constructed in a number of different embodiments, a set of embodiments for each of the various methods of changing the index of refraction. Furthermore, for any given choice of variable refraction material and appropriate energizing means there are two distinctive methods for implementing the principle of variable-refraction deflection. Variable refractors utilizing these two methods will be referred to as refractors of the first and second kinds. Refractors of the first kind utilize homogeneous materials with refractive indices that can be varied electrically. Refraction in these devices occurs at the surfaces through which the light is transmitted. Refractors of the second kind utilize homogeneous materials which are rendered slightly inhomogeneous by electrical means. For these devices refraction occurs in a continuous fashion as the light is propagated through the material. It will be shown later that the amounts of deflection which can be produced by the two kinds of refractors are substantially the same. These two kinds of refractors are described in the following subsections, and examples are given of electro-optic and elasto-optic forms of these devices.

2.1.1 Refractor of the First Kind

The variable refractor of the first kind is illustrated in Fig. 1. It consists of triangular prisms of a suitable variable-refraction material with optically flat, polished surfaces, assembled together to form a long rectangular bar. The beam of light to be deflected is transmitted lengthwise through the structure so that it passes through all of the interfaces between the prisms. Means are provided for causing the indices of refraction to vary in response to electrical signals to produce a change of index of refraction at each interface. For example, referring to Fig. 1, the lower line of prisms could have index of refraction $n_o - \Delta n$ and the upper line $n_o + \Delta n$, where Δn is a change of refractive index produced by electrical means. Alternatively, the index of refraction for one of the lines of prisms could be varied by Δn and the index for the other held to a constant value of n_o, in which case half as much deflection would be produced.

The path of a light beam through this structure is represented in line AJ. The light impinges upon the first prism in the line AB parallel to the axis of the structure and perpendicular to the left surface of the

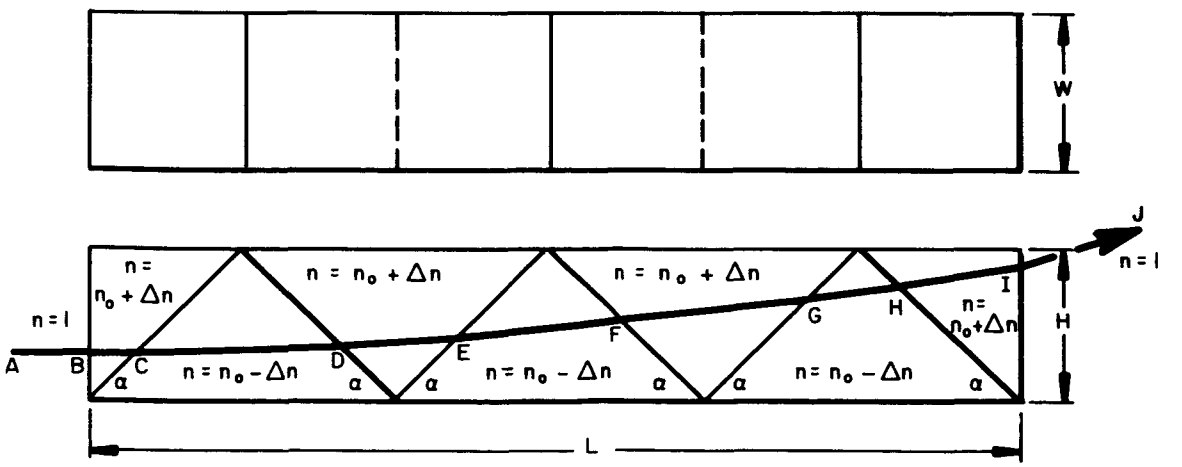

Fig. 1. Variable refractor of the first kind.

first prism. It continues in the same straight line to the interface between the first two prisms, where it is deflected slightly upward along the line CD. This occurs because it is passing into a medium of lower refractive index, causing the light to be deflected away from the normal. In passing out of the second prism, it is again deflected slightly upward, traveling in the third prism along the line DE, tilted toward the normal because of the increased refractive index. Thus, each successive refraction adds a small upward deflection. A relatively large upward deflection occurs at I where the light passes out of the structure into the air. This deflection is larger because of a much greater change of refractive index at this surface.

Two examples are given of practical forms of this refractor in the following subsections. The deflection characteristics of these refractors are discussed in Section 3.

Electro-optic refractor (first kind). An electro-optic light beam refractor device of the first kind is illustrated in Fig. 2. The prisms are single crystals of a suitable electro-optic material, such as KH_2PO_4. The index of refraction is caused to vary by application of electric fields in a direction perpendicular to the triangular faces. To achieve the desired effect, we make this the (001) direction of the crystal axes. Positive fields in this direction cause n to increase for light polarized in the $(1\bar{1}0)$ direction (horizontally), and negative fields cause it to decrease. For the crystal orientation used in this example, the index for light polarized in the (001) direction (vertically) is unaffected by the field. Light propagated at some intermediate polarization is split into horizontal and vertical components; the horizontal component is deflected, and the vertical is not. These are the ordinary and extra-ordinary rays associated with birefringence in this material.

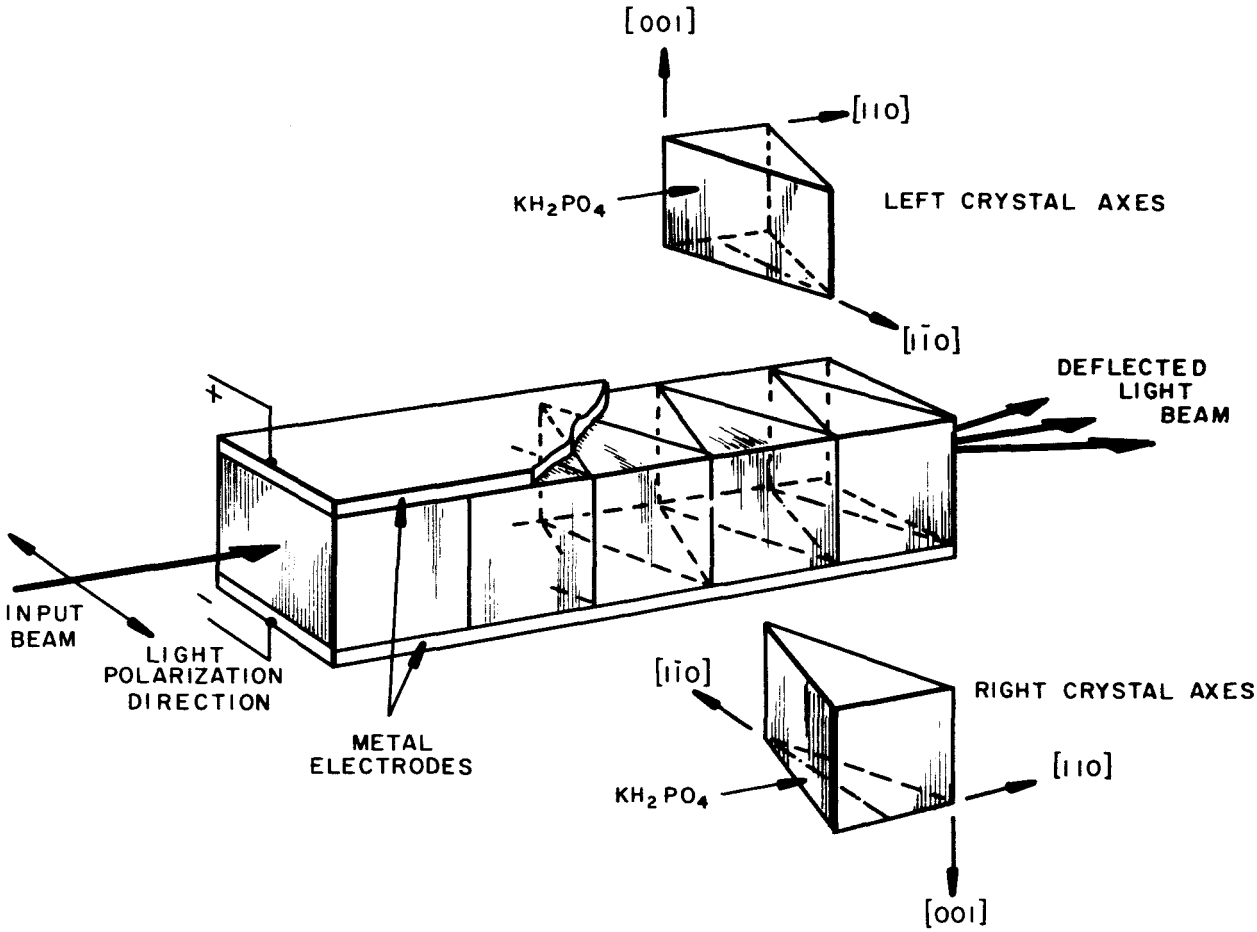

Fig. 2. Electro-optic light-beam refractor (first kind).

The indices of refraction of the left prisms are made to vary in the opposite direction from those of the right prisms by having the (001) axes oppositely directed in the left and right prisms. Thus, application of a positive voltage to the upper electrode produces a positive field in the (001) direction of the right crystals but a negative field in the (001) direction of the left crystals, and these fields have opposite effects upon the indices of refraction.

Both the left and the right prisms are the same structure and can be substituted one for the other by merely turning it upside down. A practical deflector would need only this one kind of crystal. The short

end crystals can be replaced by a suitable liquid, such as transformer oil, and this same oil can be used between the crystals to insure intimate contact; good contact is paramount to avoid total internal reflection of the light, as would happen in some cases if an air gap were present between the crystals. The transformer oil would also serve to enhance the insulation and to protect the KH_2PO_4 crystals from evanescence or deliquescence, as would occur in air that is too dry or too moist. Experimental results on structures of this type are presented later in this report.

Elasto-optic refractor (first kind). An elasto-optic refractor of the first kind is shown in Fig. 3. In this structure the refractive index of half of the prisms, the row to the right of the input beam, is caused to vary, while the prisms on the left have a constant refractive index. The prisms can be made of any one of a variety of materials exhibiting strong photoelastic effects, such as plastics, glasses, or crystals. A particularly good material is a transparent bakelite plastic, presently marketed under the trade name "Catalin." Equal uniform stresses are applied to the right prisms by means of a piezoelectric stack transducer, clamped to the prisms by a rigid steel yoke. The left prisms are made slightly shorter than the right ones so that they remain unstressed. The application of forces to the prisms in the y direction, as shown, sets up stresses in the prism in the x and z directions as well as in the y direction. These transverse stresses are smaller by a factor γ, the Poisson ratio, and they also give rise to changes in the refractive index of the stressed prisms. The total change of refractive index is the superposition of the effects of the three stress components.

For isotropic elasto-optic materials, such as Catalin plastic, the changes in refractive index produced by mechanical stresses are different for light polarized in the stress direction from what they are for light polarized transverse to the stress direction. This effect, called stress birefringence, causes the deflection angles for light polarized in the

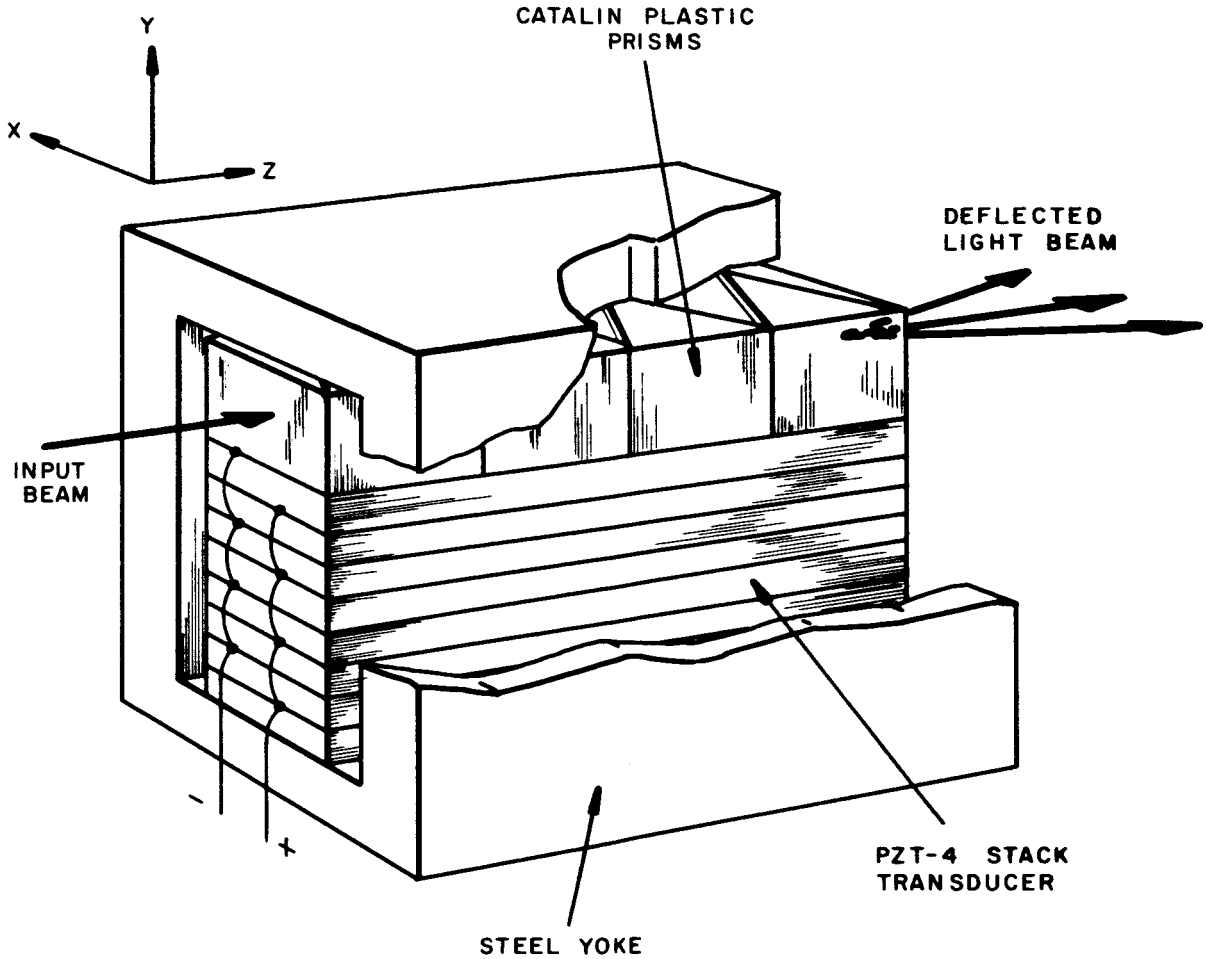

Fig. 3. Elasto-optic light beam deflector (first kind).

x and y directions to be different. Light polarized in some other direction is split into x and y polarization components, which emerge from the deflector as two separate beams at the deflection angles for x and y polarized light.

2.1.2 Refractor of the Second Kind

A variable refractor of the second kind is illustrated in Fig. 4. A single rectangular bar of variable refraction material is used, and the change of index of refraction is made to be a linear function of the distance x transverse to the light beam, as shown in Fig. 4(a). For

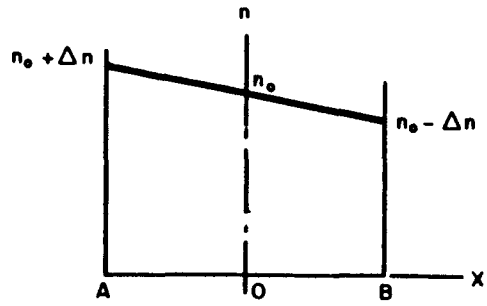

(a) Variation of n with x

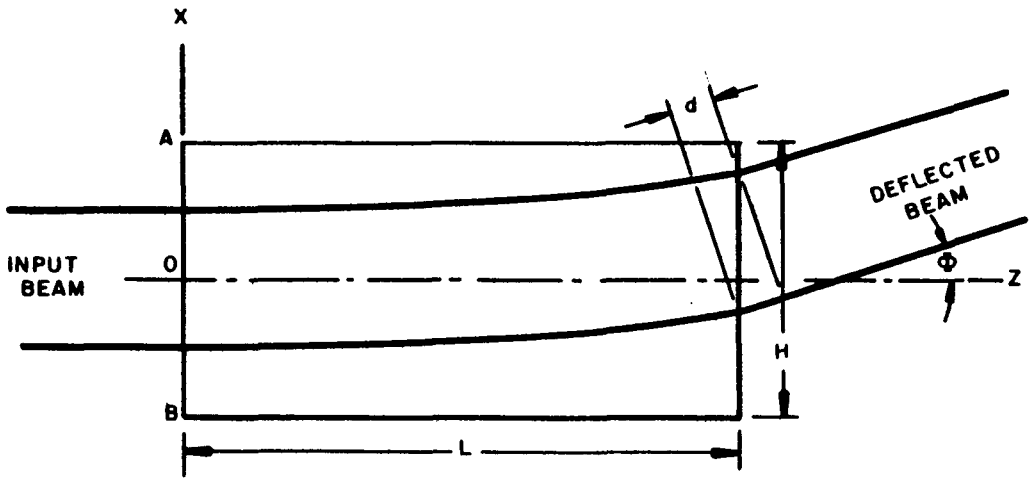

(b) Passage of light through structure

Fig. 4. Variable refractor of the second kind.

small changes of refractive index, the light rays travel in the z direction along parallel lines of constant refractive index, but because of the larger refractive index, the rays near the top travel slower than the rays near the bottom. Refraction of the entire light beam results from the fact that the relative phase velocity of adjacent rays causes a gradual tilt in the phase front of the beam as it travels down the bar. The emerging beam has a phase front tilted at the angle Φ shown.

Examples of electro-optic and elasto-optic forms of this device will now be described.

Electro-optic refractor (second kind). Linear variation of n with distance is obtained in the electro-optic refractor of the second kind, shown in Fig. 5, through the application of a nonuniform electric field to a rectangular bar of an electro-optic crystal, such as KH_2PO_4. This field is obtained with a quadrupole configuration of suitably shaped electrodes, designed to produce an electric field component in the (001) direction which varies linearly with distance in the (110) direction and is uniform in the $(1\bar{1}0)$ direction, the direction of light propagation. It is impossible to produce this field component without also producing a

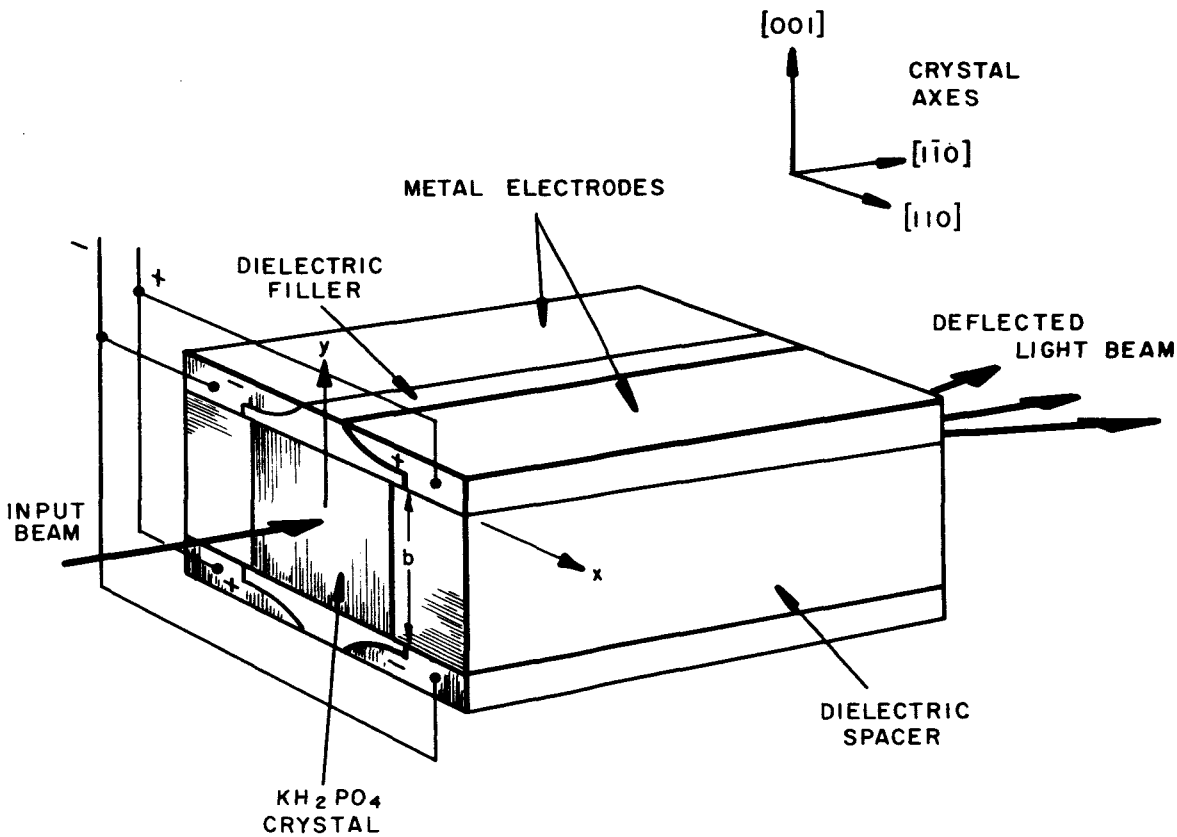

Fig. 5. Electro-optic light-beam refractor (second kind).

component perpendicular to it. The crystal orientation was chosen so that this spurious component is in the (110) direction, which is a direction for which the electro-optic effect is null. Since only the (001) component of the electric field affects n, and since n is a linear function of this field component, it follows that n also will vary linearly with distance in the (110) direction.

This structure has the advantage of not requiring large numbers of triangular electro-optic crystals, but it suffers the disadvantage that its practical construction requires a large amount of dielectric filler material which stores considerably more energy than the electro-optic crystal itself. A more important disadvantage is that the device is not capable of producing stationary deflection of a light beam. This is because the desired field pattern is obtained only if conduction current in the crystal and in the filler dielectric is zero or very small compared with the displacement current, or if the ratio of conductivity to dielectric constant is the same everywhere throughout the crystal and the filler dielectric. It appears that none of these conditions could be satisfied in a practical device. Experimental results on structures of this type developed and tested in this program are presented later in this report.

Elasto-optic refractor (second kind). An elasto-optic refractor of the second kind, shown in Fig. 6, uses two piezoelectric stack transducers in a push-pull arrangement to produce inhomogeneous stresses in a bar of a suitable elasto-optic material, such as Catalin plastic. These stresses are transmitted through a rigid steel yoke and a stiff, steel rocker plate. The structure is clamped together so that the plastic bar is under considerable compression. With one polarity of voltage applied to the transducers, the left transducer expands slightly and the right transducer contracts slightly, causing the pressure to increase on the

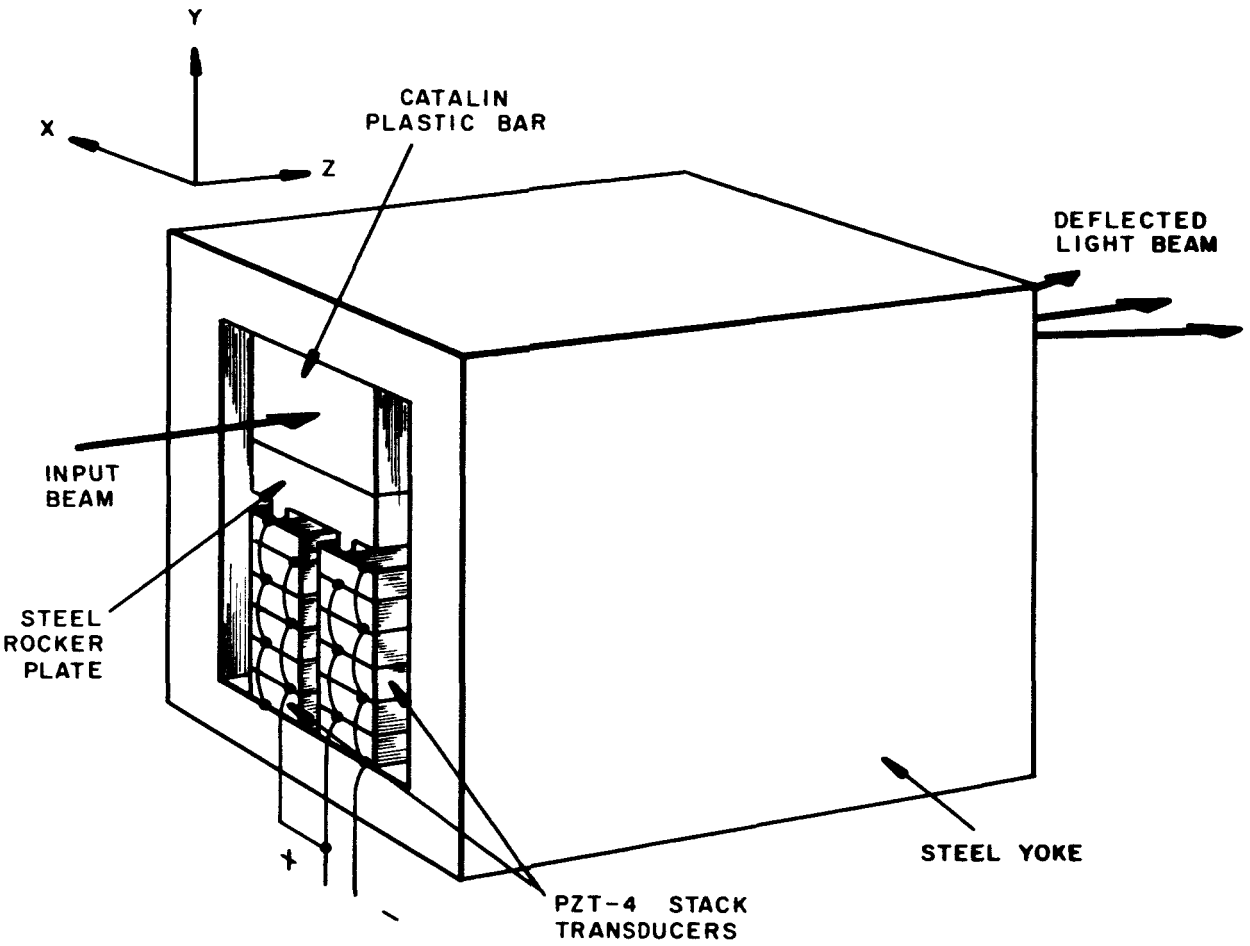

Fig. 6. Elasto-optic light-beam refractor (second kind).

left and decrease on the right. The plastic bar is then deformed slightly to the form of a trapezoidal prism. The rocker plate is rigid enough so that it maintains a flat surface in contact with the plastic bar, and as a result the vertical pressure varies linearly in the x direction. Horizontal stresses are also produced by this arrangement. They are smaller by a factor of γ, the Poisson ratio. Both the vertical and the horizontal forces are uniform in the y and z directions. Each gives rise to deflection of the light in the x direction, and the total deflection obtained is a superposition of the effects of the two stress components. Both vertically and horizontally polarized light are deflected by this device, but the amount of deflection is different for the two polarizations.

2.2 VARIABLE-DIFFRACTION DEFLECTORS

Variable diffraction can be accomplished by changing the spatial periodicity of a diffraction grating. One way to do this rapidly is to produce a grating with sound waves, varying the period of this grating by changing the frequency of the sound.

A method for doing this is shown in Fig. 7. Light from a laser is magnified and collimated to form a wide beam which is passed through a bar of a suitable elasto-optic material, such as glass or plastic. An intense sound wave is applied to one end of this bar from a piezoelectric transducer driven by a variable frequency oscillator. The opposite end of the

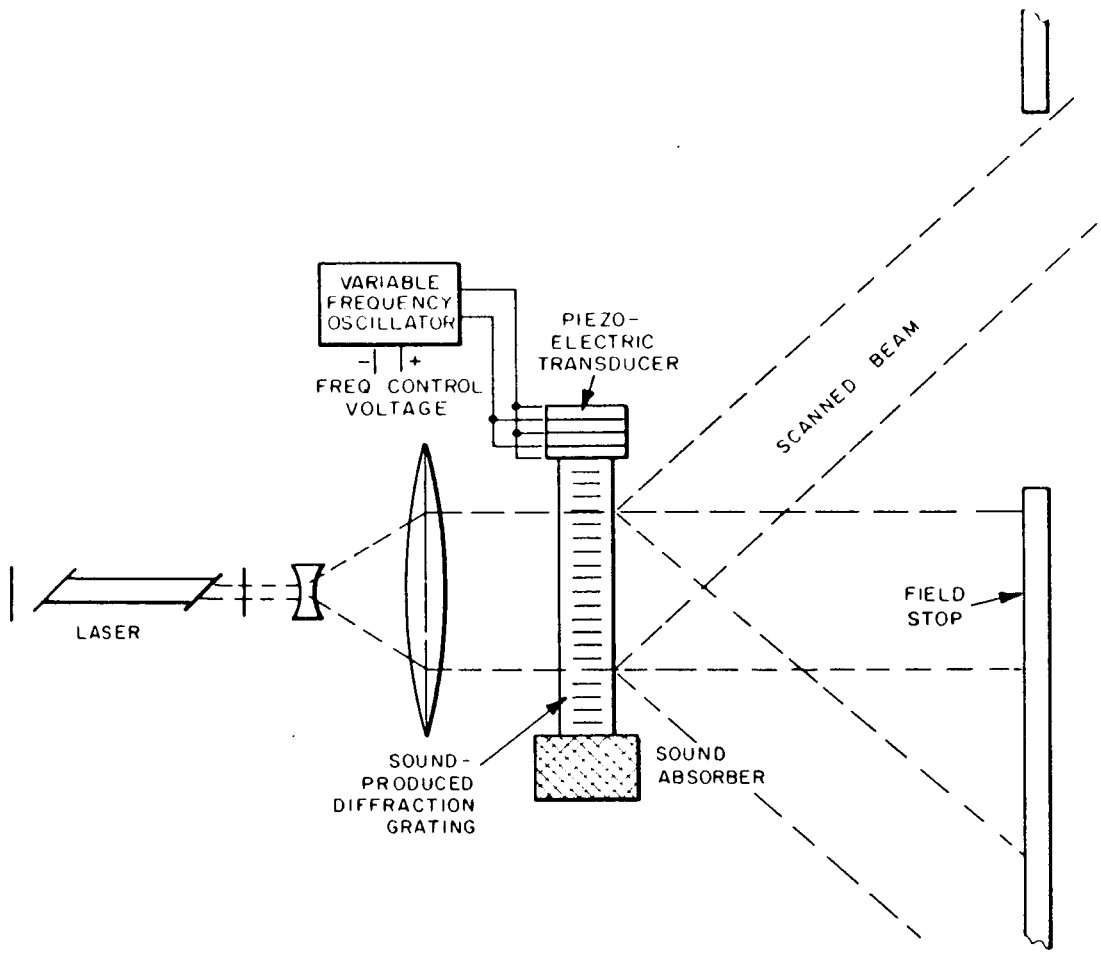

Fig. 7. Variable-diffraction deflector.

bar is terminated with a sound absorber. Therefore, the sound travels along the bar as a pure traveling wave, being totally absorbed at the far end. The refractive index of the bar is modulated slightly by the pressure of the sound wave. At a given instant of time the sound pressure, and therefore the refractive index, varies periodically with distance along the bar. Since the bar exhibits periodic optical properties, the laser light passing through the bar is split into a series of diffraction spectra. A field stop is used to remove all of the diffraction spectra, except the first-order one.

A major disadvantage of this method is the fact that high scan speeds are possible only with a severe sacrifice in scan resolution. The underlying reason for this is that high resolution requires long gratings, and the establishment of long gratings requires long periods of time. This is discussed more fully in Section 3.

2.3 VARIABLE-REFLECTION DEFLECTORS

The variable refraction and variable diffraction methods described in the previous sections can be used to achieve electrically controlled deflection without gross mechanical displacement of matter, although vibrational displacements are generated in these devices at low frequencies. Deflection by variable reflection is dependent upon production of significant amounts of displacement, and therefore this method has intrinsic limitations of frequency of response to an arbitrary deflection signal. Rotating mirrors would be incapable of meeting high-speed requirements, especially in modes of operation requiring a rapid change of rotational speed. Higher speeds could be accomplished with vibrating mirrors actuated by sonic waves from powerful piezoelectric transducers, as shown in Fig. 8. Devices of this sort could function very effectively for many applications, but they are inherently incapable of competing with the electro-optic refractor at very high deflection rates.

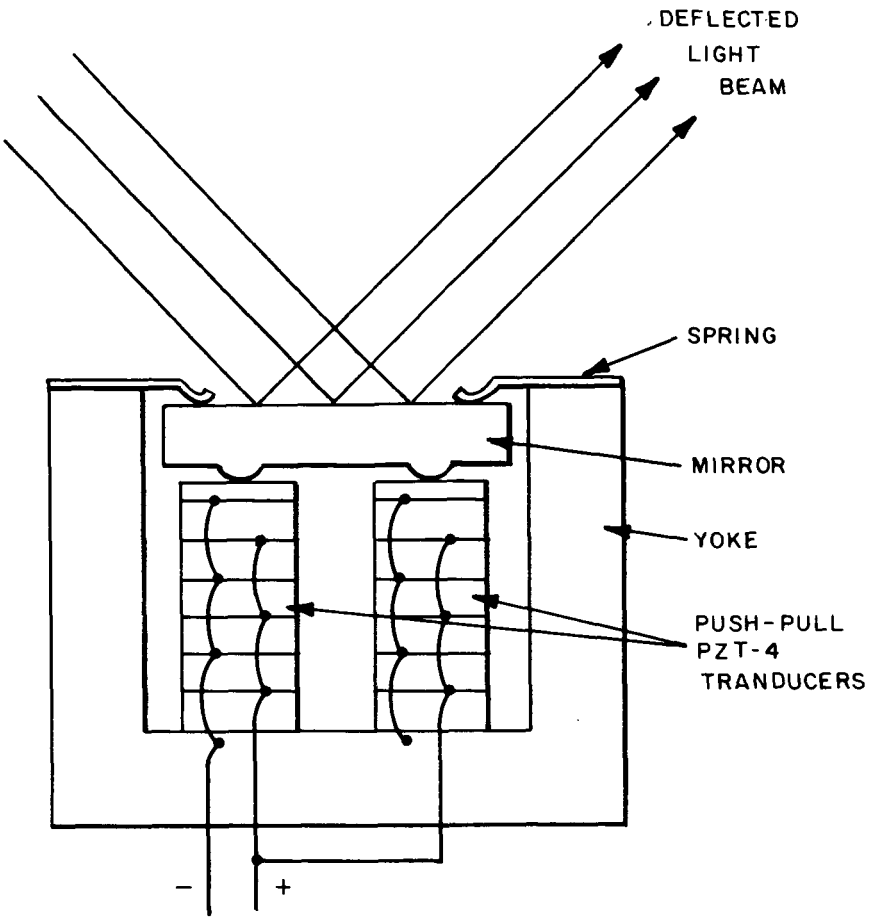

Fig. 8. Variable reflection deflector.

This can be seen from the following argument. Assume that a variable refractor like the one shown in Fig. 2 and a variable reflector like the one in Fig. 8 are both designed for optimum performance to produce equal scan angles with equal resolution at very low frequencies. The scan angle for the electro-optic scanner would be limited by breakdown voltage in the electro-optic crystal. The maximum deflection angle would then be determined by this voltage, and it would be independent of frequency. On the other hand, the maximum deflection angle for a vibrating mirror is dependent upon the maximum mechanical displacement that can be produced, and this too would be independent of frequency. The energy required

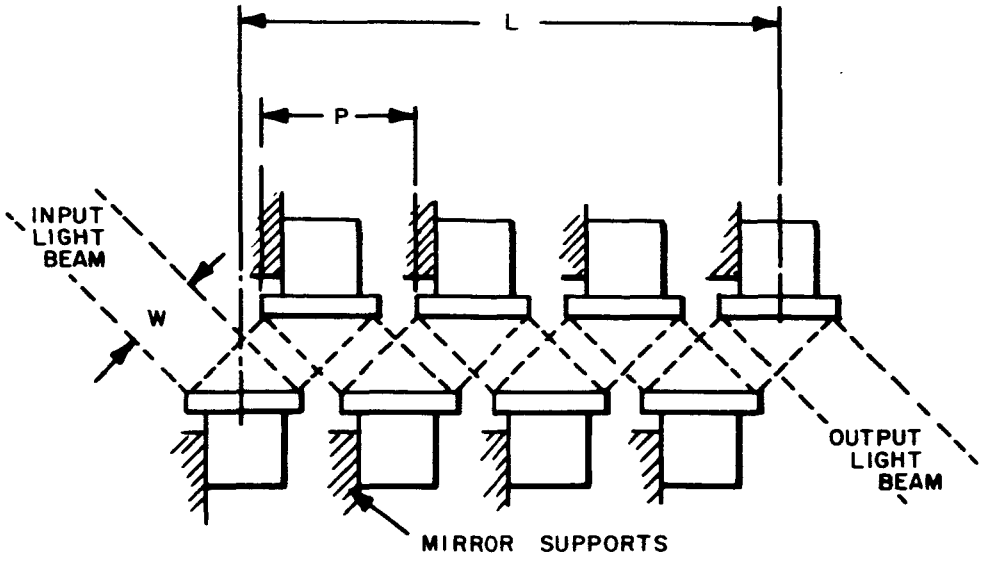

Fig. 9. Shear-plate mirror light deflector.

extraneous materials and parts which do not contribute directly to the deflection process.

The resulting simplified structure, shown in Fig. 9, consists of two parallel rows of rectangular piezoelectric prisms cemented to a double-comb supporting structure. A mirror is attached to one side of each prism, and two adjoining sides are metallized to serve as electrodes. The prisms are poled perpendicularly to the mirror surface so that application of voltage to the contacts causes shear strain in the prism, which tilts the mirror surface relative to the supporting structure. The mirrors are arranged so that the light beam threads through the structure along a zig-zag path between the parallel rows of mirrors.

to produce this maximum deflection in the electro-optic device would be proportional to the square of the voltage and still independent of frequency. The energy applied to the vibrating mirror is proportional to the square of the velocity, or the square of the time-derivative of the displacement. The peak energy would therefore be proportional to the square of the vibrating frequency. Both devices are almost non-dissipative, but there would be small losses proportional to the reactive power and inversely proportional to the system Q. The reactive power in both cases is proportional to the product of frequency and energy. Therefore, the power required for the electro-optic scanner would be proportional to the frequency, and the power required for the vibrating mirror would be proportional to the cube of the frequency. It follows then that for high enough operating frequency, the vibrating mirror will require more drive power than the electro-optic refractor. As the frequency is increased still further, the relative efficiency of the mirror will rapidly become much lower.

This argument applies only for comparison of a strongly vibrating mirror with a non-vibrating variable refractor. The piezoelectric effect causes vibrations to occur in the refractor which can be of significant magnitude for frequencies up to a few tens of kilocycles. On the other hand, it is also possible to achieve significant amounts of deflection with very slight mirror vibrations by using many vibrating mirrors in tandem. Therefore, in the audio frequency region it is quite possible to obtain more deflection with less power from a mirror device.

The obvious approach to the design of a high-frequency vibrating mirror is to make the device as small as possible. The embodiment of Fig. 8 does not lend itself to tiny construction and therefore is unsuitable. A new type of variable reflector, called a shear plate mirror (SPM) structure, was evolved in this program from successive attempts to improve the speed of response by reducing physical dimensions and removing

3. ANALYSIS OF DEFLECTOR PERFORMANCE CAPABILITIES

In this section we shall consider some of the performance capabilities and limitations of variable deflectors. Our principal concern will be with the electro-optic refractor and the shear-plate mirror, but some reference will also be made to the elasto-optic refractor and the variable diffractor.

3.1 MAGNITUDE OF DEFLECTION

3.1.1 Refractor Deflection

Expressions for the deflection angle as a function of the refractive index change are derived in Appendix A. These formulas apply only for cases where the refractive index change is very small, permitting incremental changes in deflection angle to be approximated by differential quantities. The formula of greatest interest is an approximate expression for the deflection angle Φ, accurate for small values of that angle, which applies for refractors of both the first and second kinds. That formula is

$$\Phi = 2\Delta nL/H, \tag{1}$$

where L is the total length of the structure, H is the height in the deflection direction, and Δn is the maximum change of refractive index experienced by the light beam.

In general Φ is a small angle for the attainable values of Δn, and this formula does apply. The deflection is large enough, however, to permit practical application of this device, particularly with very narrow light beams, such as can be obtained from lasers. For such sources the light can be collimated to a cone with a theoretical minimum "beam angle"

(the angle formed by the intercepts of the cone on a plane containing the cone axis) which is limited by diffraction to

$$\theta_o = \lambda_o/w, \tag{2}$$

where θ_o is more precisely the half-intensity beam angle, λ_o is the free-space light wavelength, and w is the width of the light beam as it emerges from the beam deflector.

The ratio N, defined by

$$N = \Phi/\theta_o, \tag{3}$$

is a very significant parameter. It is the number of distinguishable beam directions contained within the beam deflection angle. If the scanned beam is projected on a screen, then N is the deflection distance of the light spot measured in spot diameters. The approximate formula for N is

$$N = 2\Delta n(L/\lambda_o)\,(w/H). \tag{4}$$

At room temperature values of Δn somewhat larger than 10^{-4} can be produced by means of the Pockels electro-optic effect in crystals, such as KH_2PO_4. The limit for elasto-optic materials, such as Catalin plastic, is about ten times higher, or $\Delta n = 10^{-3}$. The length L could be conveniently as large as one foot, and w could be made practically equal to H. Thus, for visible gas laser light at $\lambda_o = 0.6328 \times 10^{-4}$ cm, we have

$$N_{max} \cong \begin{cases} 100 \text{ for electro-optic materials} \\ 1000 \text{ for elasto-optic materials.} \end{cases}$$

Still higher values may be possible in other materials, such as KD_2PO_4 (electro-optic) and $Pb(NO_3)_2$ (elasto-optic). On the other hand, the maximum value of N for magneto-optic materials is about 100 times smaller (e.g., for zinc sulfide in a magnetic field of about 2000 gauss).

It is useful to note that N also equals the number of half-wavelengths of phase retardation of one edge of the light beam relative to the opposite edge. Consider, for example, the case where w = H. The phase constant for the light passing through the variable refractor is

$$\beta = 2\pi n/\lambda_o. \tag{5}$$

Therefore, the phase shift corresponding to propagation along a distance L is

$$\theta = \beta L = 2\pi nL/\lambda_o. \tag{6}$$

The change in phase shift corresponding to the change of refractive index is then

$$\Delta\theta = 2\pi\Delta nL/\lambda_o. \tag{7}$$

The number of wavelengths of phase retardation corresponding to this change of phase shift is

$$N_{\frac{1}{2}\lambda} = \Delta\theta/\pi = 2\Delta nL/\lambda_o. \tag{8}$$

This equals N from Eq. (4) for the case w = H. It is easy to show that $N = N_{\frac{1}{2}\lambda}$ also applies for w < H.

The parameter N is much more important than the deflection angle Φ. That angle can be increased by passing the deflected beam through a magnifying lens system. However, this also magnifies the beam angle in the same proportion, and as a result N remains invariant.

Present gas lasers can produce parallel beams in a single longitudinal mode with a beam width w of about 1/8 inch. Diffraction limits the beam angle to 0.2 milliradian, or 0.012 degree. Thus, without the use of magnifying lenses, deflection angles of about 1.2 degrees can be obtained using electro-optic KH_2PO_4 crystals, and angles of about 12 degrees can be obtained using elasto-optic Catalin plastic.

3.1.2 Diffractor Deflection

The angle of diffraction produced by a grating is

$$\Phi = \lambda_o/p, \tag{9}$$

where λ_o is the light wavelength, and p is the period of the grating, which equals the sonic wavelength in the elasto-optic bar. The diffraction-limited half-intensity beam angle is

$$\theta_o = \lambda_o/W, \tag{10}$$

where W is the width of the light beam, which equals the length of the sound path along the bar. The number of distinguishable beam directions for scan angles in the range from zero to Φ is then

$$N = \Phi/\theta_o = W/p. \tag{11}$$

Thus, it is seen that this number equals the number of periods in the diffraction grating produced by the sound wave.

It is easy to get large values of N. For example, we can let W = 10 cm and p = 0.01 cm. For suitable elasto-optic materials, such as quartz or glass, wavelengths of the order of 0.01 cm are obtained at frequencies of about 50 Mc/s.

The time T_1 required to change the deflection angle Φ from one fixed value to any other fixed value is the time required for N periods to be established in the refraction grating, or N times the temporal period of the sonic wave. Thus,

$$T_1 = N/f_s. \tag{12}$$

It is necessary to re-establish the diffraction grating N times to produce a single scan line. This requires a line scan time T_L equal to

$$T_L = NT_1 = N^2/f_s. \tag{13}$$

Achievement of a two-dimensional scan of N lines with N elements per line requires a frame time T_f equal to

$$T_f = NT_L = N^3/f_s. \tag{14}$$

Therefore, for a given maximum sonic frequency f_s and a given scan rate, $f_f = 1/T_f$, the maximum attainable resolution N in elements per scan line is

$$N = (f_s/f_f)^{\frac{1}{3}}. \tag{15}$$

Figure 10 is a plot of N versus f_s for a scan frequency of 30 frames/second. It is seen that the resolution increases very slowly as the sonic frequency increases. The maximum frequency at which suitably intense sound waves can be produced for this application is about 30 Mc/s, for which N = 100. Thus, it appears that the variable diffractor is not

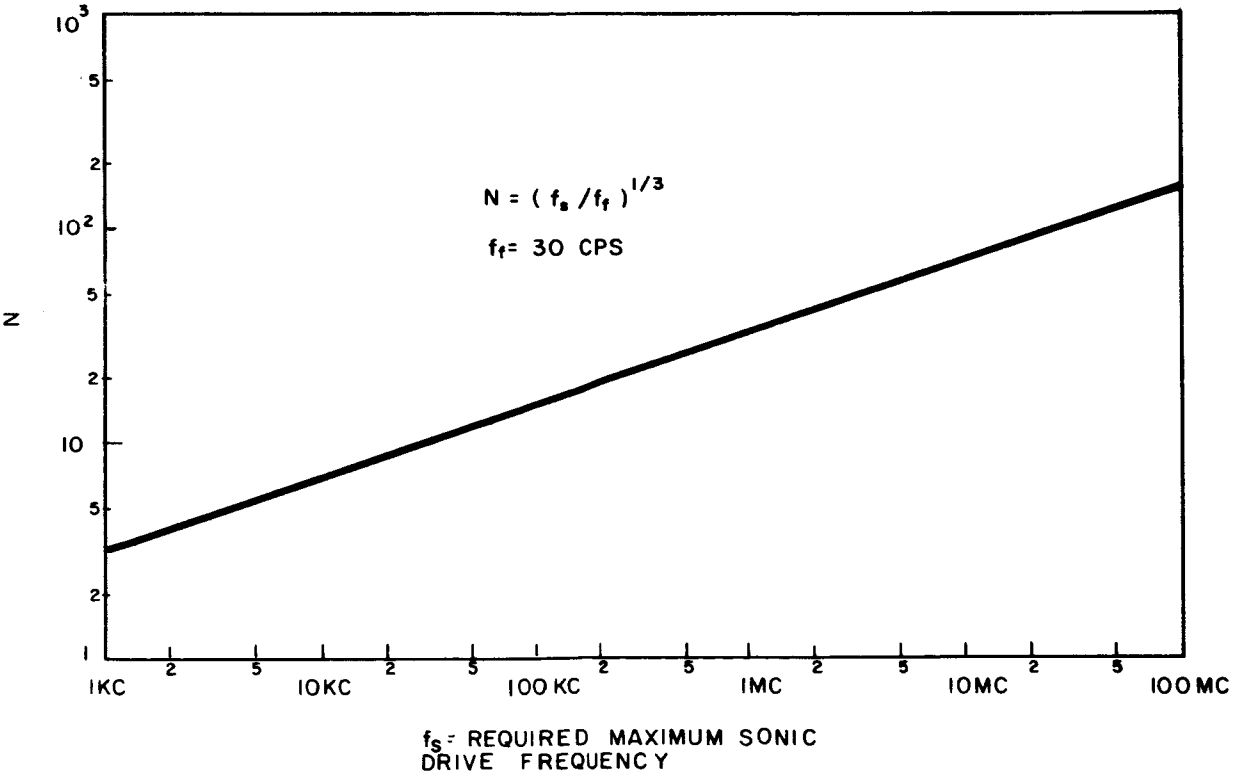

Fig. 10. Resolution of variable diffractor.

capable of very high resolution, and in fact, is not at all competitive with any of the other methods previously discussed. The resolution also becomes much worse for higher scan rates. For example, N drops to 10 when the scan rate is increased to 30 kc/s.

Further discussions concerning diffractor devices in this report will be somewhat limited because, for reasonably large values of N, the speed of response is much too slow for this device to be competitive with even purely mechanical deflection means. However, brief comments are presented in the following sections concerning other characteristics of this device.

3.1.3 Reflector Deflection

The angular change in a right angle is defined as shear strain.[1] Shear strain can be generated piezoelectrically by application of an electric field to a uniformly poled bar of piezoelectric ceramic material in a direction perpendicular to the poling direction. The magnitude of shear strain generated in this way is

$$\gamma = d_{15} E, \tag{16}$$

where γ is the deformation shear angle, shown in Fig. 11, resulting from application of the field E, and d_{15} is the piezoelectric strain constant of the piezoelectric material.

Referring to Fig. 9, we find that the number of mirrors m in a multimirror device is related to the effective deflector structure length L and the spatial periodicity P by

$$m = 1 + 2L/P \cong 2L/P. \tag{17}$$

---

1. M.M. Frocht, Photoelasticity, Vol. I, John Wiley, N.Y., 1962, p. 25.

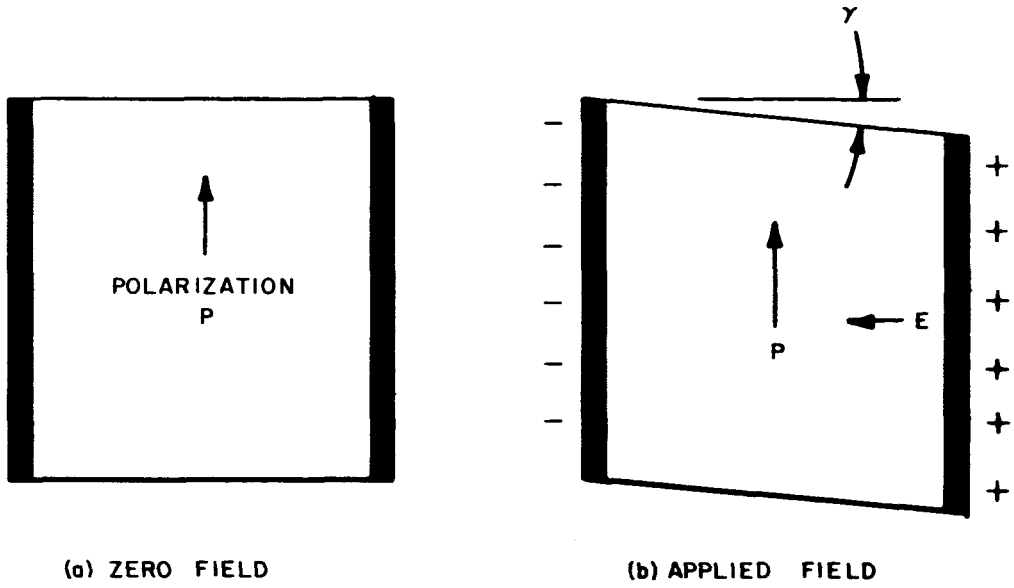

Fig. 11. Generation of shear strain in poled piezoelectric ceramic by application of electric field.

The total deflection angle is

$$\Phi = 2m\,\Delta\gamma \cong 4\,\Delta\gamma\,L/P, \tag{18}$$

where $\Delta\gamma$ is the change of shear angle induced by the applied field. The factor two appears because both the angle of incidence and the angle of reflection are changed in equal amounts by the shearing angle, and the deflection angle change equals the sum of the changes of those two angles.

From Eqs. (2), (3) and (18) it follows that the maximum number of beam positions for this structure is given by

$$N = 4\Delta\gamma\,(L/\lambda_o)(w/P), \tag{19}$$

where w, as before, is the width of the input light beam.

Values of $\Delta\gamma$ about equal to 10^{-3} can be obtained in the best piezoelectric ceramic materials (e.g., lead zirconate-titanate). The period P can be made slightly smaller than twice w. Taking the length L to be one foot and $\lambda_o = 0.6328 \times 10^{-4}$ cm, we have

$$N_{max} = 2000.$$

This is a factor of twenty larger than the deflection obtainable using the electro-optic effect in KDP and a factor of two larger than deflection with plastic elasto-optic materials.

3.2 LINEARITY OF DEFLECTION

3.2.1 Refractor Linearity

Intrinsic causes of nonlinearity were studied for variable refractors of the first kind. For these structures the maximum deflection angle equals α, the base angle of the triangular electro-optic prisms. For deflection angles approaching α, the deflection is larger than that predicted by Eq. (1). Expressions for large-angle refraction in this structure are derived in Appendix A.

Figure 12 shows the deflection angle φ as a function of a parameter u for various values of the prism base angle α. The parameter u is defined as

$$u = \frac{4m\Delta n}{n_o} , \tag{20}$$

where m is the number of lower prisms through which the light has been deflected. This family of curves can be interpreted in two different ways. For a fixed value of m (that is, a fixed location along the structure) the curves show how the deflection angle varies with Δn. Alternatively, for a fixed value of Δn the curves show how the deflection varies with distance along the structure, represented by m. It is seen that the deflection is a very nearly linear function of Δn, except for values of φ approaching α.

The curves of Fig. 12 do not show the total deflection obtained from the structure, because they do not account for the refraction produced as the light passes out of the last prism into the air. A family of curves showing the total deflection angle Φ of the emerging light is presented in Fig. 13

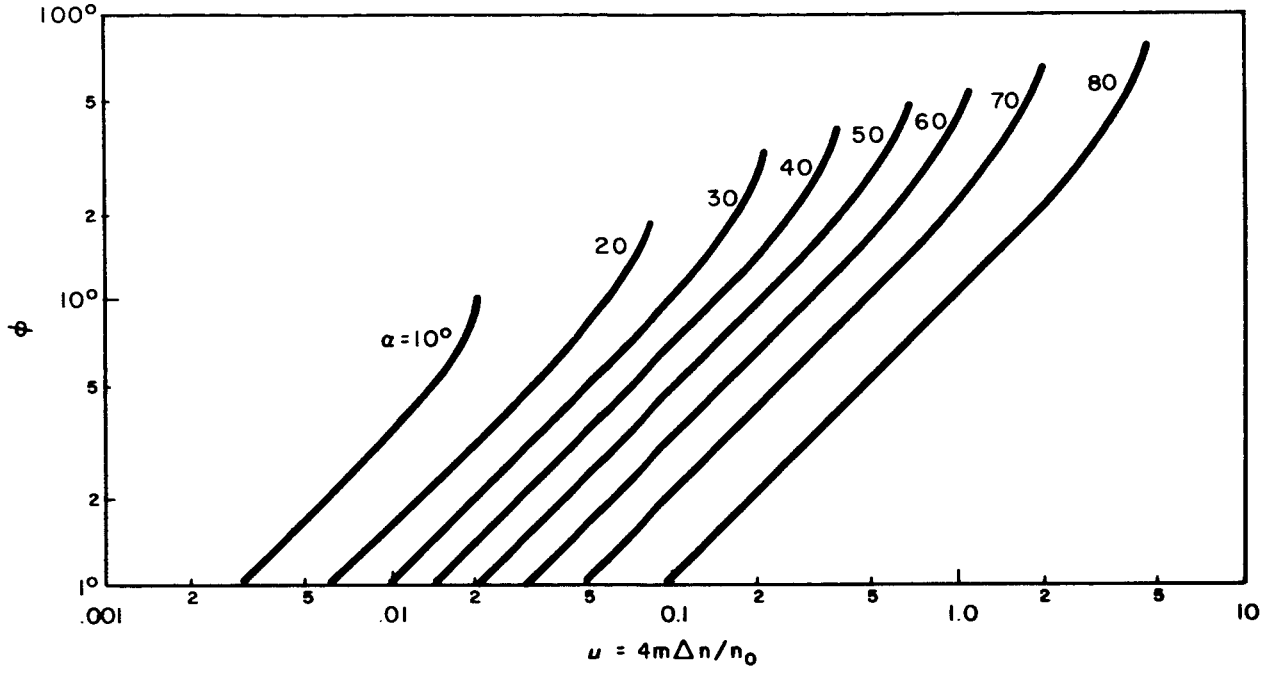

Fig. 12. Deflection vs distance along variable refractor of first kind.

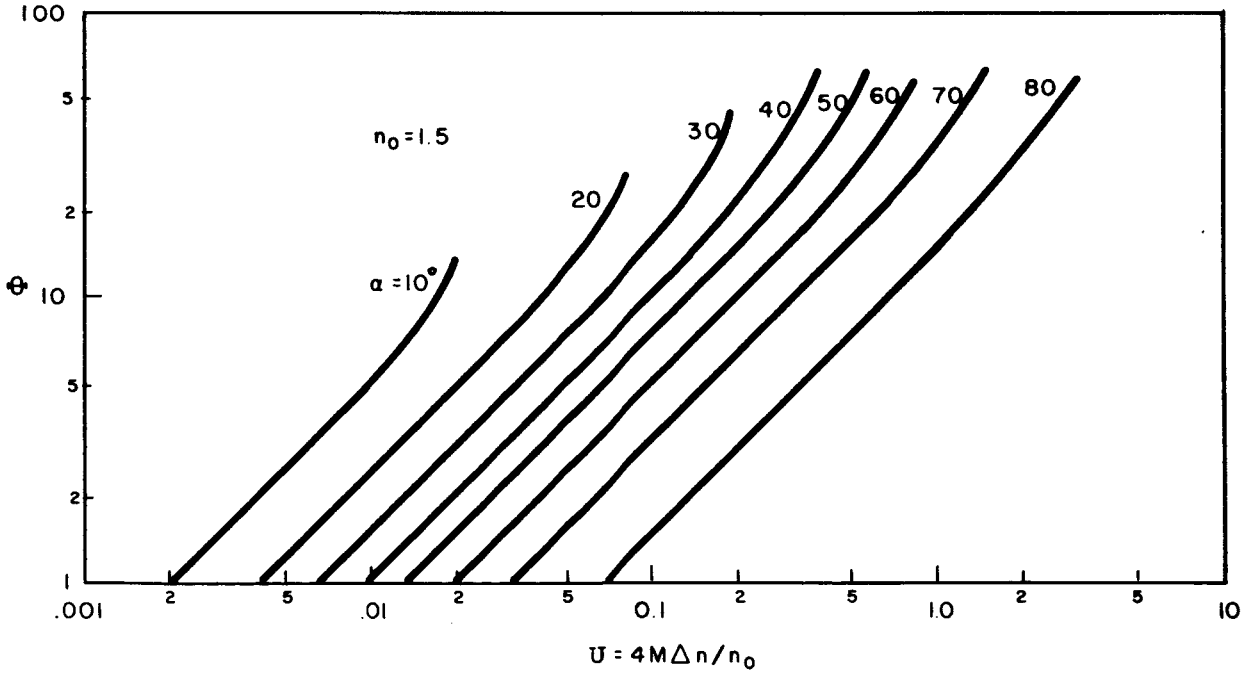

Fig. 13. Output light deflection characteristic for variable refractor of first kind.

for the case $n_o = 1.5$. The argument for these curves is

$$U = \frac{4M\Delta n}{n_o}, \tag{21}$$

where M is the total number of lower prisms. The deflection angles are increased by a factor of about n_o by the final refraction.

The deflection linearity of electro-optic refractors is also affected by the linearity of the electro-optic effect itself. Comprehensive data are not available on the variation of refractive index of electro-optic crystals in very strong electric fields. These data are most readily obtained by refraction measurements on the beam deflector device itself. Therefore, further discussion of nonlinearity is postponed until Section 4 in which measurements of the linearity of deflection are presented.

3.2.2 Diffractor Linearity

The deflection linearity of variable refractors is determined by two factors: the linearity of the relationship between frequency and frequency control voltage for the variable frequency oscillator of Fig. 7 and the linearity of the relationship between that frequency and the wave number 1/p (i.e., the non-dispersiveness of the plane sound wave in the sound-produced grating). By careful design, the sonic line could probably be made substantially non-dispersive, and one would expect that the main source of nonlinearity would reside with the oscillator. It appears that it would be very difficult and expensive to produce a variable frequency oscillator with accurately linear frequency control characteristics over a large relative frequency range. This is a second reason for rejecting the variable-diffraction method for use in precision high-speed laser beam deflection.

3.2.3 Reflector Linearity

Piezoelectric ceramics are ferroelectric, having a hysteresis loop curve of polarization versus electric field. The shear strain is directly proportional to the polarization, and therefore the strain versus applied voltage curve is also a hysteresis loop. Linearity of deflection in the shear plate mirror can be expected to be quite good for small deflections, but it should get quite nonlinear at fields large enough to produce depoling. The extent of nonlinearity of this sort can be determined only by measurement, and this measurement is most conveniently performed on an actual shear-plate mirror deflector device. Data of this sort are presented in Section 4 for deflectors utilizing barium titanate and lead zirconate-titanate ceramics.

3.3 POWER REQUIREMENTS

3.3.1 Refractor Power

For electro-optic variable refractors of the first kind, the electrical energy density in the structure (neglecting fringe fields) is

$$W_e = \tfrac{1}{2} \epsilon_1 E^2 \qquad (22)$$

where ϵ_1 is the dielectric constant of the crystal in the field direction, and E is the applied field. Most existing electro-optic materials have relatively large dielectric constants, and the fields required to achieve maximum values of Δn are extremely high. For example, for KH_2PO_4 the relative dielectric constant is 20, and the maximum field that can be applied without breakdown is about 30 kv/cm. Using fields ranging from +30 kV/cm to -30 kV/cm, one can obtain a maximum refractive index change of $\Delta n = 10^{-4}$ peak-to-peak. This is obtained with an energy density in the crystals of about 8×10^{-4} joule/cm^3.

The power requirements for a structure with W = H = 0.2 inch and L = 12 inch are plotted in Fig. 14 versus the scan frequency. A field of 30 kV/cm is assumed, for which the scan voltage is 15 kV and the deflection is about one degree peak-to-peak.

The dashed curve is for a linear sweep, assuming that 10 percent of the scan cycle is utilized for retrace. The power requirements for a linear scan are dictated by losses attendant upon generation of the driving voltage. For example, if a Miller sweep circuit is used, losses will be encountered in the vacuum tube generating the sweep and in the plate load and feedback resistors. For these calculations an ideal Miller sweep was assumed, for which the theoretical minimum power dissipation is $2V_sI_s$, where $2V_s$ is the peak-to-peak scan voltage and I_s is the scan current. A maximum sweep power of 50 watts might be considered acceptable for most applications. This sets the maximum operating frequency for this design at about 1 kc/s. This frequency could be extended almost an order of magnitude by reducing the cross-sectional dimensions and increasing the length, using larger numbers of crystals.

Because of this rather high energy density, it is very important to minimize the crystal volume so that the total stored energy is low, allowing operation at high frequencies with reasonable amounts of driving power. The width and height of the prisms should be about equal to accommodate round laser beams. Manufacturing difficulties with the individual prisms presently limit W and H to about 0.2 inch. This is a fairly convenient size, because it provides an aperture which accommodates the usual gas laser beam without the need for input optics. The length is set by the required deflection angle, or by the required resolution. For a deflection angle of about one degree (corresponding to a maximum deflection resolution of about 100 beam diameters), a length of about 12 inches is required. This makes the

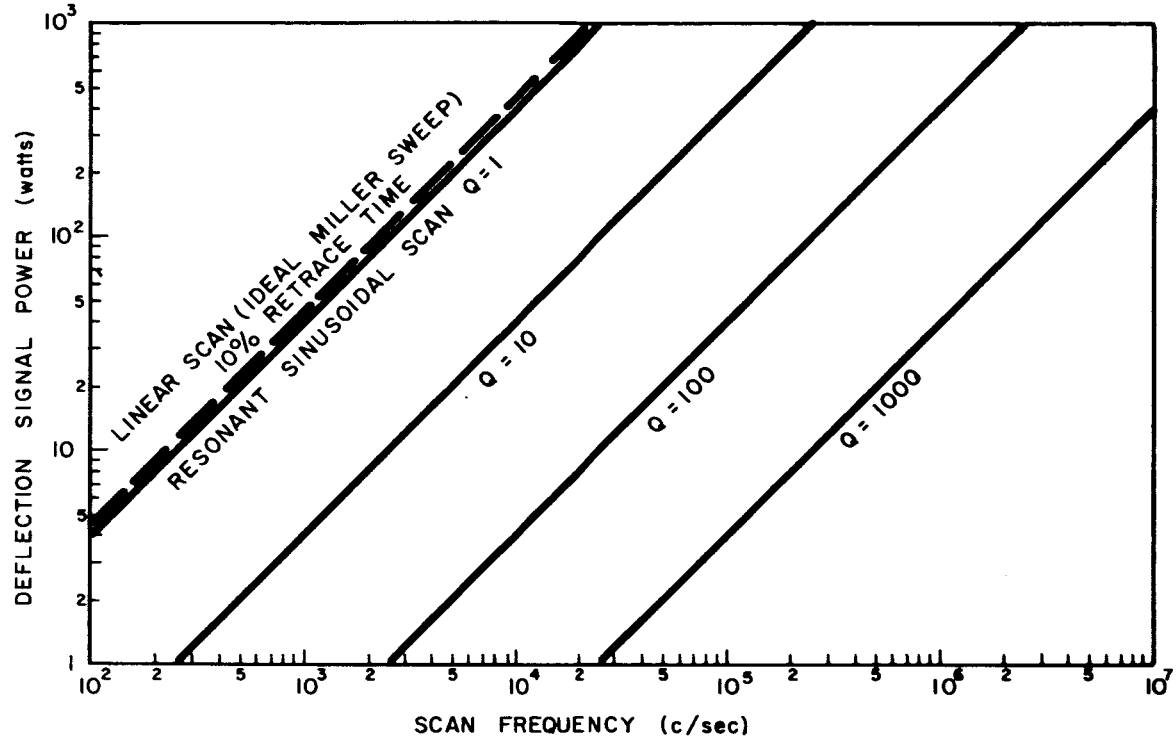

Fig. 14. Power requirements for an electro-optic scanner of the first kind (not acoustically resonant).

total crystal volume about 8 cm^3 and the total maximum stored energy about 6.4×10^{-3} joule. The total number of crystals is sixty, each crystal contributing a deflection of about 0.016 degree.

The solid curves of Fig. 14 show the power requirements for sinusoidal scans using scan voltages derived from resonant circuits. The scan power is determined by losses in the resonant system, which are inversely proportional to the system quality factor Q. Plots are given for Q = 1, 10, 100, and 1000. Values of Q of the order of a few hundred can be obtained at frequencies in the range from 10^4 to 10^6 c/s. It can be seen from the figure that scan rates up to about 300 kc/s can be used with 50 watts of power. The maximum scan frequency is increased by a factor slightly larger than the system Q.

In the foregoing discussion it is tacitly assumed that the electro-optic refractor crystals are not acoustically resonant at the scan frequency. Acoustic resonance can drastically affect both the power requirements and the magnitude of deflection. It appears that with proper design it should be possible to utilize acoustically generated strains to increase the scan angle and decrease the scan power. This effect was not studied during this program, but it is now under investigation in the extension of this program under Contract NAS 8-11459.

3.3.2 Reflector Power

Under maximum field conditions the stored energy density in a piezoelectric ceramic is considerably larger than that in an electro-optic crystal. In the previous section we found that the maximum energy density in KH_2PO_4 is about 8×10^{-4} joule/cm^3. The most suitable piezoelectric ceramic for use in a shear plate mirror is lead zirconate titanate, which has a dielectric constant of about 1475 and a maximum allowable applied

field of 10 kV/cm. Its maximum energy density is eight times greater than that for KH_2PO_4, or about 6.4×10^{-3} joule/cc. On the other hand, one shear plate mirror can generate much more deflection than one refractor prism, even though both have to be about the same size to deflect a light beam of a given diameter. Deflection angles of about 0.1 degree are attainable with a lead zirconate titanate shear cube, whereas deflection from a single refractor prism is six times smaller. Therefore, one needs only one sixth as many shear-plate mirrors, and consequently the power requirements can be roughly the same.

This comparison assumes that the ceramic piece has to be about as large as the mirror and that it must be a cube. It should be possible to use relatively small piezoelectric elements to drive relatively large mirrors, thereby reducing the power requirements for non-resonant operation. Reducing the size of the shear plate, however, decreases the area of contact with the mirror, weakening the cemented bond and preventing operation at high frequencies for which inertial forces exerted on this bond by the vibrating mirror are excessive.

It should be noted that direct comparison of driving power may be much less significant than a comparison of operating voltages, because high power can be obtained much more conveniently, inexpensively, and compactly at low voltages than at high voltages. A good comparison can be made between the refractor design cited in the previous section and a reflector using ten quarter-inch shear-plate cubes of lead zirconate titanate. The reflector requires 2.5 times as much stored energy to achieve the same deflection as the refractor, but it operates at about 0.4 times the voltage, or about 6.3 kV. Furthermore, this voltage could be reduced by a factor of five or so by making each shear plate in the form of a stacked piezoelectric transducer, consisting of , say, five plates each

1/4 inch square and 0.05 inch thick. Interleavened electrodes could be used to furnish the same field with an applied voltage of 1200 volts. This sort of thing could not be done with a refractor, because interleavened electrodes would interfere with passage of the light beam through the structure.

3.4 LIGHT INSERTION LOSS

3.4.1 Refractor Light Loss

The curves of Figs. 12 and 13 all show that the deflection is quite linear when the deflection angle is much less than the prism base angle α. In the linear region Φ is given by Eq. (1), which is independent of α. Therefore, all values of α are equally good as far as deflection sensitivity is concerned. However, practical variable refractors of the first kind require films of oil between the crystal faces to prevent total internal reflection. This oil can be selected to provide a refractive index close to the index of the crystal. A particularly good choice for α is 45 degrees. This makes the angle of incidence of the light on the crystal-oil interface very close to the Brewster angle, given by

$$\theta_p = \tan^{-1}(n_1/n_2), \tag{23}$$

where n_1 is the refractive index of the crystal, and n_2 is the index of the oil.

Reflection losses for light polarized in the plane of incidence were calculated for variable refractors of the first kind. For these calculations it was assumed that each passage of the light beam into and out of the oil is accompanied by a reflection light loss which is independent of all of the other reflection losses. This ignores the possible interferences among

the various reflections. This is a reasonable approximation, because the interferences are as likely to increase the losses as to decrease them, making the average effect of many interferences equal zero.

The calculations were made for a KH_2PO_4 structure with a height-to-length ratio H/L equal to 0.01, which is approximately the value needed to achieve a one-degree scan angle. The results are shown in Fig. 15 which is a set of plots of total reflection loss in decibels versus the number of base crystals $M = L/L_1$, where L_1 is the base length of each prism. The curves are for $n_1 = 1.51$ (the index for the ordinary ray in KH_2PO_4) and $n_2 = 1.0$, 1.5, and 1.6. A scale at the top shows the corresponding values of the base angle α.

The curve for $n_2 = 1$ shows zero light loss for $M = 75$, for which α is the Brewster angle (56.5 degrees), and rapidly increasing light loss either side of this value. For $n_2 = 1.5$ reasonably good match is obtained so that the light loss is less than 0.1 decibel everywhere in the range from $M = 30$ to $M = 150$ and higher, corresponding to α in the range from 30 to greater than 70 degrees. For $n_2 = 1.6$ the loss is less than 0.1 decibel in the range from $M = 40$ to $M = 60$, corresponding to α in the range from 50 to 60 degrees.

It is concluded from this that reflection light losses can be made negligible, even for very long structures involving many individual prisms. The base angle α is not critical, and it can be set equal to the convenient angle of 45 degrees. For this choice the value of n_2 is also not critical, but it should not be smaller than n_1.

3.4.2 Reflector Light Loss

The source of light loss in a shear-plate mirror deflector is absorption of light by the mirrors. The light loss in decibels for a M-mirror device is

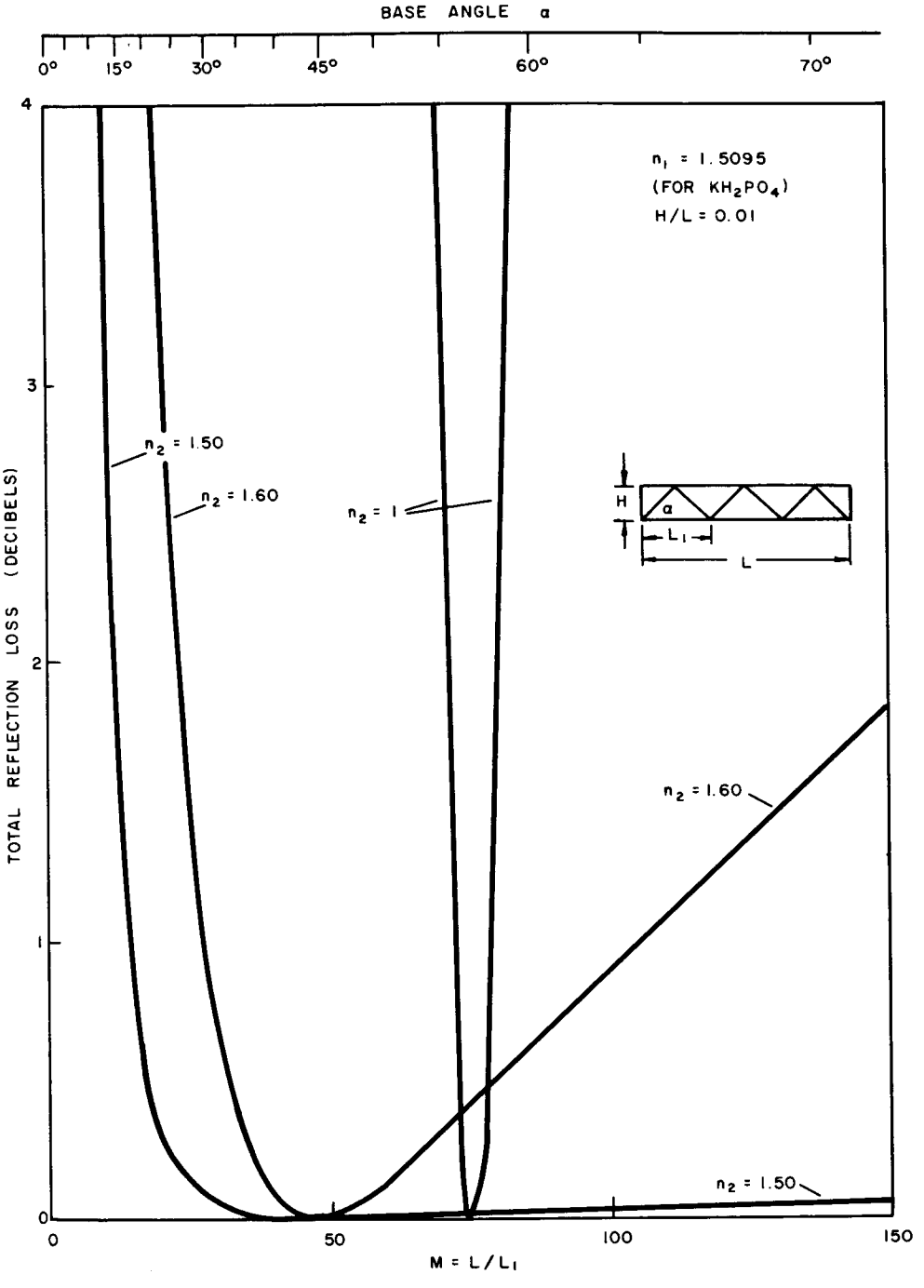

Fig. 15. Reflection losses of variable refractor of the first kind.

$$L = 10\,M \log_{10} R \qquad (24)$$

where R is the reflectivity of a single mirror. This function is plotted in Fig. 16 for various values of reflectivity. For a silvered glass front-surface mirror the reflectivity at 6328 Å is about 0.93. This produces a total light loss of about one dB in only three reflections, and a loss of over 3 dB in ten reflections. Much lower reflection losses can be obtained by using multilayer dielectric mirrors of the sort used in gas laser cavities, for which reflectivities of about 0.995 are readily achieved. Fifty or more of these mirrors can be used in a deflector structure with a total light loss of about one dB.

3.5 LIGHT-BEAM PHASE-FRONT DISTORTION

3.5.1 Refractor Distortion

Refractors of the first kind will generate nonuniform phase retardation if the electric fields within the triangular prisms are not uniform. Refractors of the second kind will produce distortion if the field is not a linear function of distance across the beam. For both kinds of refractors, distortion will occur if the crystal surfaces through which the light passes are not flat and properly oriented.

The distortion consists of two components: a zero-field component which is independent of the applied field, and an induced component which exists only in the presence of the field. For example, lack of flatness in a rectangular prism in a refractor of the second kind generates both zero-field and induced distortion. The surface curvature produces a lensing effect which is present even when there is no voltage applied. This effect, fortunately, can be minimized by using oil to fill in the space not occupied by the crystals. By choosing the oil to have a refractive index matching

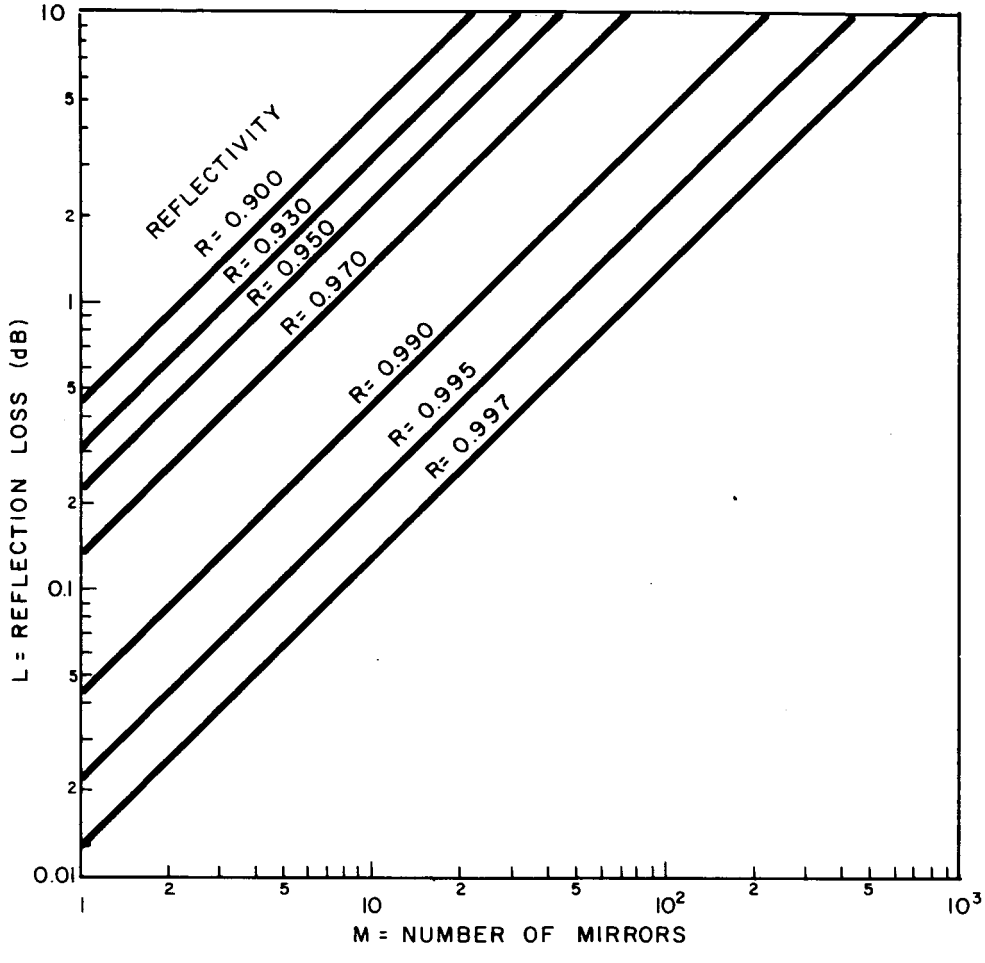

Fig. 16. Reflection light loss in shear-plate mirror deflector vs mirror reflectivity.

the index of the electro-optic crystal, one can make the crystal surfaces invisible in the oil. The lack of flatness also causes the total effective length of the crystal to be different for different rays in the light beam, and this can cause individual rays to be retarded by incorrect amounts, yielding a form of field-induced distortion. This effect is not eliminated by the presence of the oil; however, the effect is small because it is proportional to the change of refractive index rather than to the refractive index itself.

The zero-field effects of surface roughness and/or curvature can be estimated in the following way. It is assumed that light passes through P interfaces between electro-optic crystals of refractive index n_x and a fluid (e.g., oil or air) of refractive index n_o. The surface flatness, expressed in wavelengths of the laser radiation is F (rms value). The rms phase error generated by each interface is then

$$\Delta\theta_1 = 2\pi(n_x - n_o)F. \tag{25}$$

For the P statistically independent passes through interfaces of the same roughness, the total rms phase error is $(P)^{\frac{1}{2}}$ times larger, or

$$\Delta\theta_t = 2\pi P^{\frac{1}{2}}(n_x - n_o)F. \tag{26}$$

Surface irregularities enlarge the laser beam by scattering. It takes a linear phase variation of π radians across a laser beam to shift that beam by about one diameter. Therefore, one can expect scattering to be just barely detectable if the rms phase variation equals about $\pi/7$ radians. This corresponds to a root-mean-square departure of the wave front from its correct position equal to 1/14 of a wavelength. This is Marechal's criterion for flatness for a well-corrected optical system.[2]

2. M. Born, E. Wolf, Principles of Optics, Pergamon Press, N.Y., 1959, p. 468.

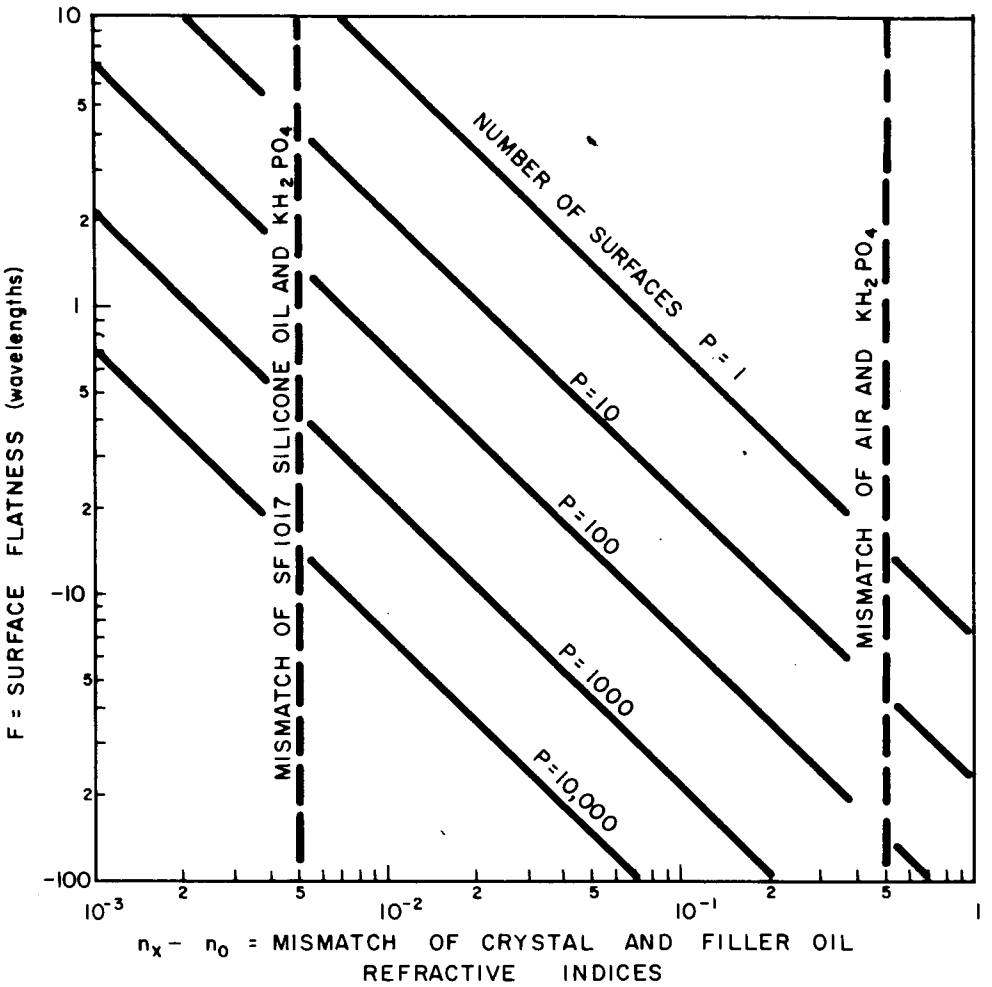

Fig. 17. Required surface flatness for electro-optic crystals in refractor.

Using this value of $\pi/7$ radians for $\Delta\theta_t$, the required surface flatness has been plotted versus $n_x - n_o$ for various values of P, shown in Fig. 17. Vertical dashed lines are drawn in this figure for the ordinates corresponding to mismatch of KH_2PO_4 with air and with SF-1017 silicone oil. A surface flatness of about 0.1 wavelength can be obtained on water-soluble crystals, such as KH_2PO_4. It can be seen from the figure that detectable distortion would occur from one or two passes of light through a polished crystal into air, whereas thousands of passes would be required to generate the same amount of distortion if the silicone oil were used between crystals.

The field-induced effects of surface roughness and/or curvature is given by an expression identical to Eq. (26), except that $n_x - n_o$ is replaced by Δn, the field-induced change of refractive index. This quantity is much less than 10^{-3} for known electro-optic crystals; therefore, it can be seen from Fig. 17 that the field-induced mismatch of refractive index produces completely negligible distortion, provided that the crystal surfaces are flat to within a few wavelengths.

Distortion generated by errors in the field distribution within the electro-optic crystals is difficult to analyze, except for a few simple cases. One example is the error caused by application of the wrong deflection voltage. If the deflection (as viewed by projecting the beam on a distant screen) is supposed to be 100 spot diameters and the maximum allowable error is 0.14 of a spot diameter, then the applied voltage must be correct to within 0.14 percent. A second example is lack of parallelness of the triangular faces of the electro-optic prism in a refractor of the first kind, causing unequal deflection of different portions of the beam. To maintain deflection constant to within 0.1 spot diameter with a total deflection of 100 spot diameters, one must maintain parallelness of the electrode faces to within 0.0014 radian, or 4.8 minutes. This accuracy is very easy to

achieve. In general, one would expect that deflection accuracy of 0.14 percent will require dimensional tolerances of about this same magnitude, i.e., 0.14 percent.

3.5.2 Reflector Distortion

The zero-field component of distortion in the shear-plate mirror deflector results entirely from irregularities in the mirror surfaces. These effects cannot be reduced or eliminated, except by making the mirror surface flatter. About an order of magnitude of increased flatness is possible in hard, stable optical materials, such as quartz, compared with the flatness that can be obtained from electro-optic crystals. For a multiple mirror structure the rms phase distortion will increase in proportion to the square root of the number of mirrors. Each mirror can be made about twenty times flatter than is required to satisfy Marechal's flatness criterion; therefore, up to a few hundred mirrors can be used in a shear plate deflector structure before this component of distortion becomes appreciable.

Field-induced distortion can occur if the mirror is bent by the piezoelectric ceramic cube while it is being tilted. Such distortion can occur if the cube experiences some longitudinal strain in addition to shear strain, which will happen if the polarization direction is not perpendicular to the field direction in the cube, or if the polarization and/or field are not uniform. These effects can be eliminated by making the bond between the ceramic cubes and the mirrors somewhat elastic. In addition, the effect can be reduced by making the mirrors relatively thick so that they resist bending forces.

3.6 STABILITY

3.6.1 Refractor Stability

The main source of instability in electro-optic refractors is the temperature dependence of the electro-optic effect in crystals. Changes of temperature cause changes of deflection sensitivity, and this changes the amount of deflection in proportion to the magnitude of that deflection. The electro-optic constant r_{63} has a temperature dependence which follows the Curie-Weiss law[3]

$$r_{63}(T) = r_{63}(T_1)\frac{T_1 - T_o}{T - T_o} \tag{27}$$

where $r_{63}(T)$ and $r_{63}(T_1)$ are the values of the electro-optic constant at the given temperature T and some other reference temperature T_1, and T_o is the Curie temperature. For a small temperature change, $\Delta T = T - T_1$, the relative change in r_{63} (hence the relative change in deflection angle) is

$$\frac{\Delta r_{63}}{r_{63}} = \frac{\Delta T}{T - T_o}. \tag{28}$$

For KH_2PO_4 the Curie temperature T_o is 122°K. Therefore, at a room temperature of 300°K, a temperature change of one degree causes a deflection change of 0.56 percent, or half a spot diameter for a total deflection of 100 spot diameters. It is apparent that stable deflection of this magnitude calls for stabilization of the crystal temperature to within less than 1/2 degree. Stable deflection of a hundred spot diameters also calls for very good stability of the driving signal source. For accuracies of one quarter of a spot diameter, the driving signal must be accurate to within 1/4 percent.

---

3. F. Seitz, D. Turnbull, Solid State Physics Vol. 4, Academic Press, N. Y., 1957, pp. 14, 15 and 90.

3.6.2 Reflector Stability

Instability in the shear-plate mirror structure can arise from temperature dependence of the piezoelectric effect and from slow spontaneous depolarization of the piezoelectric ceramic elements.

The temperature dependence can be quite different for different ceramic materials. Published data on the shear strain coefficient d_{15} versus temperature are not available, but they can be expected to be quite similar to the data for the compressive strain coefficient d_{31}. Figure 18 shows typical curves of d_{31} versus temperature for two lead zirconate titanate ceramics manufactured by Clevite Corporation. The curves are quite dissimilar, having room-temperature slopes of opposite sign and differing in magnitude by a factor of four. The smaller slope is for PZT-4, which happens also to be the better material for operation at high stress levels. If the coefficient d_{15} for this ceramic is as nearly constant as d_{31}, then the deflection angle for a PZT-4 shear-plate mirror would change about 0.1 percent for a one degree temperature rise.

This change is about six times smaller than the corresponding figure for a KH_2PO_4 refractor structure. Therefore, it appears that the shear-plate mirror structure can have temperature stability comparable to that of a refractor structure. There is also the possibility of altering the composition of the ceramic to minimize the temperature coefficient of d_{15}, or to make it zero at room temperature.

It is well known that piezoelectric ceramic materials are subject to aging effects. For example, the dielectric constant of PZT-4 will decrease about 7 percent during the first 100 weeks after poling, and the dielectric constant of PZT-5 will decrease about 0.3 percent in the same time.[4]

4. D. Berlincourt, B. Jaffe, H. Jaffe, H. Krueger, "Transducer Properties of Lead Titanate Zirconate Ceramics," Clevite Corporation.

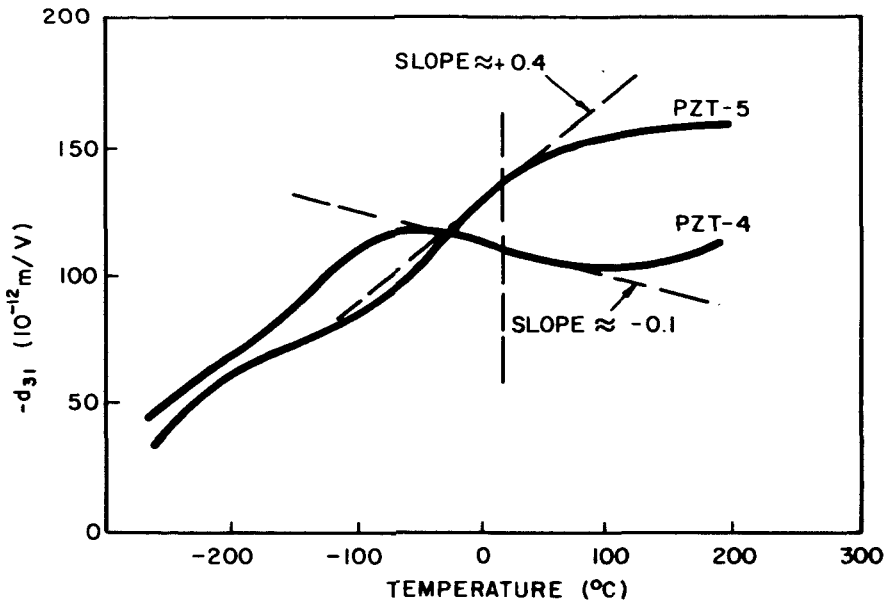

Fig. 18. Typical curves of piezoelectric constant d_{31} vs temperature for two Clevite lead zirconate titanate ceramics.

Application of very high electric fields also produces depolarization. It is likely that the presence of strong fields would accelerate the aging process. This requires further investigation before the shear-plate mirror is considered for use as a precision deflector.

4. EXPERIMENTAL INVESTIGATION OF DEFLECTOR DEVICES

4.1 DEVELOPMENT OF EXPERIMENTAL DEFLECTOR MODELS

A total of ten experimental deflector models were constructed under this program: four electro-optic refractors of the second kind (EOR2 models), three electro-optic refractors of the first kind (EOR1 models), and three shear-plate mirror deflectors (SPM models). These models are listed in Table I along with some of the design parameters for each structure.

In all of the electro-optic refractor models the choice of crystal size was a compromise between the optimum size, which was two or three times smaller, and the size of the crystal most conveniently and economically fabricated, which was somewhat larger. Triangular crystal prisms of KH_2PO_4 were purchased in two different sizes from two vendors. The larger crystals, 0.3 x 0.3 x 0.6 inch, were the smallest that could be obtained ground and polished to our specifications. They were made by Isomet Corporation. The smaller crystals, 0.2 x 0.2 x 0.4 inch, were obtained from Clevite Corporation as oversize blanks. Techniques were developed in these Laboratories for polishing the small crystals while the larger crystals were on order. Finished crystals of both sizes were completed early in the program, and EOR1 models were made with both the large and small crystals. The EOR2 models all used rectangular crystals 0.125 x 0.250 x 1.000 inch, made by Clevite Corporation.

TABLE I

Laser Beam Deflector Models

Model No.	Prism dimensions (inches) L	W	H	No. of prisms	Active length (inches)	Max. defl. angle (degrees)	Min. beam angle (degrees)	Prism material
EOR2-1	1.000	0.250	0.125	10	10.0	0.50	0.0114	KH_2PO_4
EOR2-2	1.000	0.250	0.125	5	5.0	0.25	0.0114	KH_2PO_4
EOR2-3	1.000	0.250	0.125	10	10.0	0.50	0.0114	KH_2PO_4
EOR2-4	1.000	0.250	0.125	18	18.0	0.9	0.0114	KH_2PO_4
EOR1-1	0.400	0.200	0.200	20	4.0	0.25	0.0071	KH_2PO_4
EOR1-2	0.600	0.300	0.300	20	6.0	0.25	0.0047	KH_2PO_4
EOR1-3	0.600	0.300	0.300	20	6.0	0.25	0.0047	KH_2PO_4
SPM-1	0.250	0.250	0.250	10	3.4	0.50	0.0081	Body 21
SPM-2	0.250	0.250	0.250	8	2.6	1.0	0.0081	Body 31
SPM-3	0.250	0.250	0.250	8	2.6	1.0	0.0081	Body 31

The shear-plate mirror structures all used 0.250-inch piezoelectric ceramic cubes, poled for shear. Model SPM-1 used ten cubes of Body 21 barium titanate ceramic, made by Gulton Industries, attached to 0.250-inch-square, 0.125-inch-thick quartz front-surface mirrors. Models SPM-2 and SPM-3 each used eight cubes of Body 31 lead zirconate titanate ceramic, also made by Gulton, attached to 0.5-inch-square, 0.1-inch-thick mirrors.

The total lengths of most of the deflector structures were chosen for experimental convenience rather than to achieve any particular maximum deflection. The only exceptions were Models EOR2-4, SPM-2, and SPM-3, which were designed to provide a maximum deflection of about one degree.

A photograph of refractor Models EOR1-1 and EOR2-2 is presented in Fig. 19.

4.1.1 Refractor Models

The first structures to be developed were refractors of the second kind. All of these structures were constructed as a number of separate one-inch-long deflector cells mounted in tandem on four L-shaped brass rails and installed in hermetically sealed oil-filled plexiglass tubes with quartz windows. Each of the cells consisted of a rectangular KH_2PO_4 electro-optic crystal, a two-piece quadrupole electrode structure, two plexiglass spacers, and two nylon screws to hold all of these parts together. The spacers are individually ground to the same thickness as the crystal with a tolerance of +0.0005 inch and -0.0000 inch. Mounted alongside the crystal, they allow the electrodes to be screwed in position around the crystal without stressing the crystal.

Fig. 19. Two electro-optic deflector models, EOR1-1 and EOR2-2.

The hyperbolic electrodes were formed by milling a brass block with a special circular cutter formed to the proper shape. The space milled out was then filled with an epoxy cement with a fairly high dielectric constant and high dielectric strength. The epoxy used in these structures was Stycast 2651, manufactured by Emerson and Cumming Corp. which has a dielectric constant of 4.4. An excess of this cement was applied, and the milling cuts were made a few mils deeper than required; a final machining cut finished both the brass and the epoxy to the proper dimension and provided a flat surface to contact the crystal and spacers.

The formula for the hyperbolic electrodes, derived in Appendix B, is

$$y = -bK_2/2K_{y1} + (X_1/x)(Y_1 + bK_2/2K_{y1}),$$

where y is the depth of cut, x is transverse distance, X_1 and Y_1 are the coordinates of any point on the hyperbola (which can be selected arbitrarily), K_2 is the dielectric constant of the filler dielectric, K_{y1} is the dielectric constant of the crystal for fields in the y direction, and b is the thickness of the crystal in the y direction. The parameters used for these models were as follows: $X_1 = 0.100$ in., $Y_1 = 0.005$ in., $K_2 = 4.4$, $K_{y1} = 20$ (for KH_2PO_4), and $b = 0.111$. The cutter extended from $x = -0.100$ in. to $x = +0.100$ in. so that it generated a pair of hyperbolic surfaces simultaneously. Before the hyperbolic surfaces were milled, the brass electrode blocks were hollowed out from behind the electrode surface and the void was filled with epoxy. The milling cut that formed the hyperbolic surfaces also cut through the brass and into the epoxy underneath, thereby electrically isolating the two hyperbolic electrodes from each other.

The electro-optic refractors of the first kind were constructed after the first two structures of the second kind had been completed. The EOR1 models are of a very simple design. Two rows of 10 triangular KH_2PO_4 crystals were used in each assembly. The crystals were furnished with

metallized electrode surfaces (silver paint for Model EOR1-1 and gold plating for Models EOR1-2 and EOR1-3), and the surface corresponding to the positive z axis of the crystal was labelled with an identifying dot. One of the two rows of crystals had the dots facing up, the other had the dots facing down, and the two rows were interlaced to form a long trapezoidal prism. The crystals were installed in this configuration in a trough comprising a brass bottom plate and two plexiglass sides attached with nylon screws. The trough was covered by a brass strip in the form of an oblong ring. Phosphor bronze springs, screwed to the ring and projecting through the hole, contacted the top triangular surfaces of the individual crystals. The bottom triangular surfaces made contact with the brass bottom plate.

A great deal of attention was devoted to the cleaning, assembling, and oil-filling operations to keep the insulating oil in the structures and the electro-optic crystals completely free of all contamination, including dirt and moisture. All machined parts were cleaned chemically and ultrasonically to remove dirt and loose particles. The filling oil was obtained fresh from sealed bottles. After filling the structure, any residual water vapor and dissolved air was removed by pulling a vacuum on the envelope, using a flexible hose connection to a high-vacuum pump. Much shaking and turning of the envelope was necessary to release air trapped in screw holes and between mating parts. This operation takes several hours of manual attention in addition to an overnight pumpdown. The final pressure obtained was usually about 10^{-6} torr. After removal of the hose, the remaining space in the envelope was filled with oil from a dropper, and the fill hole was plugged.

In spite of the cleaning precautions, significant quantities of very fine brass powder appeared in some of the structures after many hours of operation, occasionally collecting in a strong field region and causing a

short circuit. It was discovered that these particles were coming from the epoxy used to fill the hollowed-out brass blocks. The particles were firmly embedded in the epoxy during a grinding operation, and were pulled out of the epoxy by the very strong deflection signal fields. This difficulty was corrected in later models by substituting a milling operation for the grinding operation.

The EOR1 structures were also installed in plexiglass envelopes, which were filled with insulating oil and hermetically sealed with rubber O-ring seals. These structures, unlike the EOR2 models, were left assembled for a period of over six months, retaining the same oil fill and the same gaskets. In this period of time the oil acquired a yellow color, and vision through the structure became obscured. Chemical analysis revealed that the O-rings had been attacked by the silicone oil. The yellow coloring was from a yellow emulsion in the oil formed by the chemical action on the rubber. This emulsion had deposited on the surfaces of some of the crystals. However, it was found that the crystals could be wiped clean without damaging the optically polished surfaces. Teflon O-rings have been ordered to replace the rubber ones in all of the refractor models.

Experiments were made with several different oils in the refractor structures to reduce light loss and provide maximum dielectric strength. The first three structures, EOR2-1, EOR2-2, and EOR1-1, were filled initially with SF-1017 methyl phenyl fluid, manufactured by General Electric Silicone Products Department. This oil has a refractive index of 1.495. As an experiment to test the idea of matching refractive index with oil, the first structure, EOR2-1, used crystals with fine ground but unpolished ends. Very good distortionless transmission was obtained with all of the structures, but there was a significant amount of light attenuation, as follows:

Model No.	Transmission loss %	dB
EOR2-1	25	6.0
EOR2-2	51	2.9
EOR1-1	44	3.6

Refractor models EOR1-2, EOR1-3, and EOR2-3 were all filled initially with a special oil mixture which almost exactly matched the refractive index of KH_2PO_4 at 23°C. This oil consisted of 100 parts of SF-1017 fluid and 84.7 parts of XF-1059, an experimental dielectric fluid, also made by General Electric, with a refractive index of 1.540.

The recipe for this oil was arrived at experimentally, using a number of triangular crystals of KH_2PO_4 immersed in the oil as a sensitive indicator of refractive index mismatch. The oil and crystals were contained in a rectangular glass tray with the hypotenuse edges of the crystals all banked against the side of the tray. A laser beam was passed lengthwise through the tray, traveling through the crystals in succession and being refracted in the same direction by each of the crystals in turn. The amount of refraction was determined by noting the position of the output laser beam on a distant screen, then pushing all of the crystals out of the beam and observing how much the spot moved. By successive approximations, the relative error in refractive index was reduced from 2.68 percent (for the SF-1017 oil alone) to 0.015 percent for the 100:84.7 mixture.

Although this mixture provided a very good match, results with it in the deflector structure were disappointing. It was found that the light loss and the amount of forward-scattered light increased. Furthermore, the laser beam could be seen passing through the oil in the structure, even though the crystal surfaces were invisible in the red laser light. Tests were made to determine the light loss in the various oils themselves by measuring the light loss in passing a laser beam lengthwise through

a three-inch-long tray filled with oil. The results were as follows:

Oil	Transmission loss %	Transmission loss dB
SF-1017 fluid alone	65	1.85
XF-1059 fluid alone	93	0.3
100:84.7 mixture	28	5.5

Another oil mixture was also tried as a refill in structures EOR2-1 and EOR2-3 and as the original fill in EOR2-4. This was a mixture of two parts of Dow Corning Type 703 silicone oil with one part of Dow Corning Type 555 silicone oil. This mixture provided a very good refractive index match with greatly reduced absorption and scattering, but difficulties were experienced with dielectric breakdown in structures filled with this mixture. Since part of the trouble was the presence of brass particles, it was not certain that the dielectric strength of the oil was responsible. Further experience with these structures will be required to pinpoint the difficulty. In general, the most satisfactory results have been obtained using the SF-1017 oil.

4.1.2 Shear-Plate Mirror Model Development

Development of the shear-plate mirror structure was simplified by the absence of water soluble crystals and filler oils, but complicated by the need to achieve extremely accurate alignment of the mirror surfaces. An initial attempt was made to develop a structure with a built-in feature of precision window alignment. This structure used two long comb-like pieces of quartz to which are attached the piezoelectric cubes and mirrors. It was realized later that this design was impractical for a first experimental model, because the method of construction left no room for error: if any one of the cubes or mirrors was cemented on

incorrectly or if it subsequently became uncemented, there was no satisfactory way to repair the structure. Furthermore, it was very difficult to provide interconnections of the piezoelectric cubes using this type of construction.

Because of these difficulties, this structure was not completed. Instead, the shear-plate mirror deflector was redesigned for an entirely different type of construction, abandoning the feature of automatic precision mirror alignment in favor of a simpler and more reliable assembly method. Instead of the left mirrors being mounted on one subassembly and the right mirrors on another, the mirrors were all mounted on individual subassemblies of two kinds, left-handed and right-handed. These subassemblies were then mounted into the proper positions by bolting them together with a pair of thick teflon studs, interlacing left- and right-handed subassemblies and using plastic spacers in between.

The subassemblies each consisted of an L-shaped brass plate, a quarter-inch cube of piezoelectric ceramic poled for shear, a half-inch square, 0.1-inch thick quartz front-surface mirror, and a phosphor bronze leaf spring. The ceramic cubes were furnished with identifying dots on the surfaces to which had been attached temporary positive electrodes during the poling operation. The outward normal from these surfaces point in the direction of the permanent internal polarization of the cubes. The mirrors were cemented to the cubes with Type 910 cement, manufactured by Eastman Kodak Company. For the right-hand assemblies they were attached to the dotted sides of the cubes; for the left-hand assemblies they were attached to the sides opposite the dots. Either of the two electroded sides of each cube was then cemented to one of the brass plates, using a special cementing jig which held the mirror in proper orientation and position relative to the brass piece. Silver epoxy was

used between the metallized bottom surface of the cube and the brass surface, and added strength was provided with a fillet of Testor's cement along three edges of the cube. The leaf springs were attached to the brass plates prior to the cementing of the cubes, and holes were provided in the brass plates to receive the two 1/4-inch diameter teflon studs which held the subassemblies together. L-shaped plexiglass plates were sandwiched between the brass plates as insulating spacers. The leaf springs were positioned to make pressure contact with the cubes of the following subassemblies. The springs also extended beyond the plate, opposite to the cubes, and served as soldering lugs for wires which interconnected the subassemblies. Extra pairs of mirrors were used at the ends of Models SPM-2 and SPM-3 to bend the input and output light beams around so that, in the absence of a deflection voltage, these beams coincide with the axis of the structure. These deflectors were also provided with hermetically-sealed plexiglass envelopes with anti-reflection coated end mirrors. Means were provided for filling the envelopes to a few pounds of pressure with an insulating gas, such as dry nitrogen.

4.2 DEFLECTOR CHARACTERISTICS

Data on the basic characteristics of the deflector models are summarized in Table II. Both calculated and measured values are given for the deflection sensitivity (i.e., deflection angle per unit applied voltage). Calculations are based on the formulas presented earlier in this report, using data on the electro-optic crystals and piezoelectric ceramics furnished by the manufacturers. For the EOR1 models, the data agree quite well with the calculations. For three of the EOR2 models the measured sensitivities were considerably lower than the calculated values. For the SPM-2 structure the deflection was much larger than calculated, whereas for the SPM-1 structure it was smaller.

TABLE II

Characteristics of Experimental Deflector Models

Model No.	Defl. sensitivity (degrees/kV)		Max. deflection obtained		Deflector capacitance (pF)
	Calc.	Meas.	Degrees peak-to-peak	Appl. voltage (kV)	
EOR2-1	0.026	0.018	0.44	12	179.9
EOR2-2	0.013	0.011	0.27	12	89.5
EOR2-3	0.026	0.017	0.43	12	180.5
EOR 2-4	0.047	0.025	0.60	12	287
EOR1-1	0.0081	0.0082	0.25	15	38.1
EOR1-2	0.0054	0.0052	0.15	15	51.9
EOR1-3	0.0054	---	0.15	15	---
SPM-1	0.048	0.039	0.40	5.0	730
SPM-2	0.064	0.097	1.1	6.0	610
SPM-3	0.064	---	1.1	6.0	---

The fourth and fifth columns of Table II show the maximum peak-to-peak deflection angles obtained with these structures and the maximum peak deflection voltages that were applied. These are not necessarily maximum attainable values either for these designs or for these particular models. Voltage was limited in some instances to avoid breakdown from miscellaneous causes, alluded to previously. Work is continuing on these structures in the extension contract, and it is expected that much higher deflections will be obtained from the electro-optic models. Most of the crystals and subassemblies have been tested with dc voltages up to 30 kV.

The last column of Table II shows the values of deflector capacitance, measured at 1000 c/s. The capacitance of the EOR2 models should be

proportional to the number of cells. Good agreement is obtained in the measured capacitance per cell for Models EOR2-1, EOR2-2, and EOR-2-3. However, the capacitance per cell for Model EOR2-4 was about 10 percent lower. The deflection sensitivity per cell for this structure was also disproportionately low, being about 20 percent lower than in the EOR2-1 and EOR2-2 models, and 35 percent lower than in the EOR2-2 model. This discrepancy is being investigated in the extension program to determine whether the cause is error in the shape or spacing of the electrodes, or in the orientation of some of the crystals.

4.3 DEFLECTED SPOT SHAPE MEASUREMENTS

One of the major objectives of this program was to determine the capabilities of the deflector models under investigation for achieving precision controlled deflection. Toward this end measurements were made to determine: (1) to what extent the deflected beam was distorted in shape, and (2) to what extent the deflection angle was a nonlinear function of the applied voltage. A special test apparatus, called a scanning photometer, was developed as part of our Company-supported program on optical devices and used to obtain data on the detailed performance of the deflector structures under development in this program. The scanning photometer automatically generates curves of light intensity versus distance across a laser beam. It operates stroboscopically so that these curves can be generated while the laser beam is being deflected at rates from zero to about 120 scans per second. A brief description of this apparatus is given in Appendix C.

Figures 20 and 21 show data obtained with this apparatus for deflector Models EOR2-2 and SPM-1. These data are plots of light intensity along a center line passing through the light beam in the deflection direction

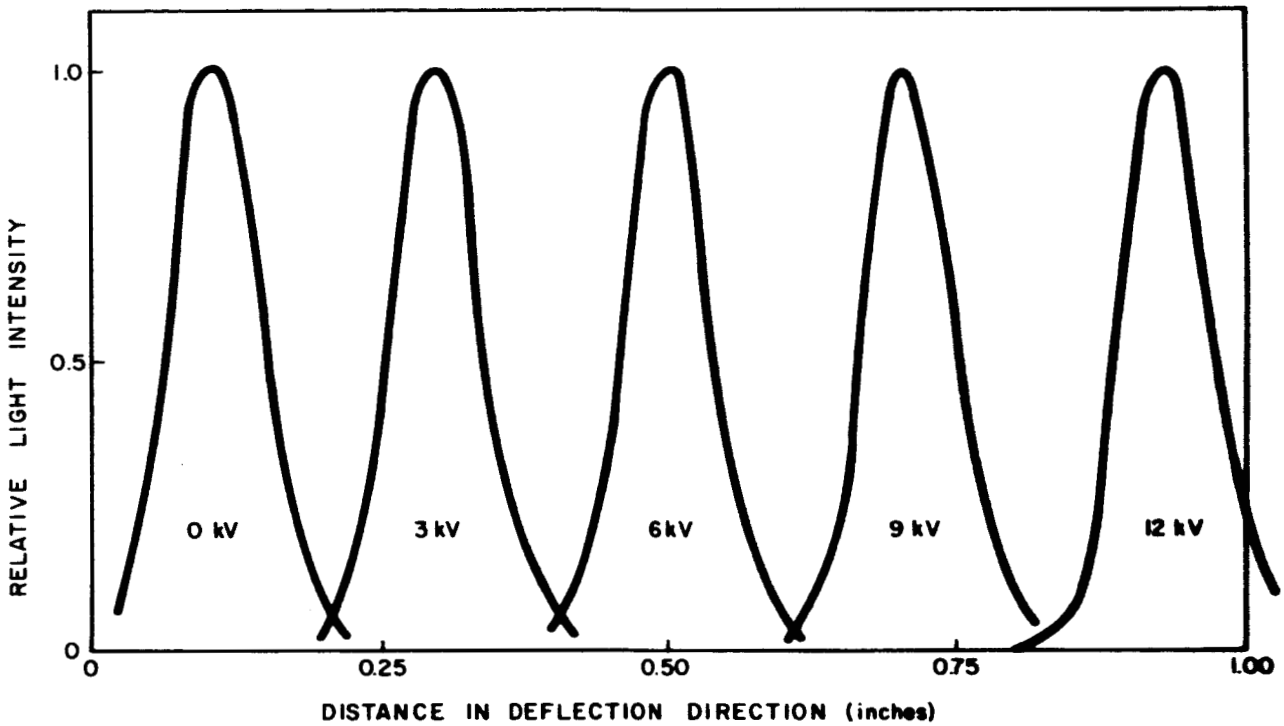

Fig. 20. Stroboscopic measurements of deflected spot shape for refractor EOR2-3.

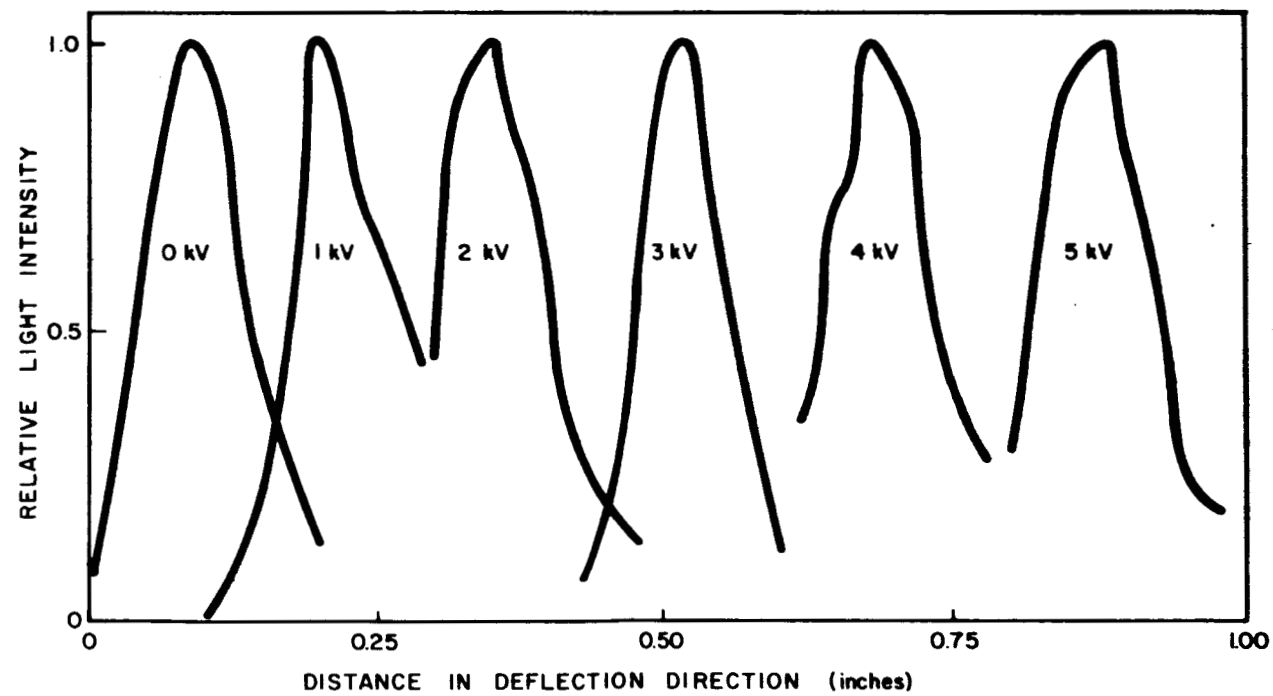

Fig. 21. Stroboscopic measurements of deflected spot shape for shear-plate mirror SPM-1.

versus distance in that direction. Each of the figures shows several such plots obtained with various values of voltage applied to the deflector. The individual plots were all normalized to a maximum value of intensity equal to unity. With this normalization, data on the effects of the applied voltage upon the center-of-spot intensity are lost; however this information was not reliable, since the laser beam varied in intensity during the data run. Furthermore, virtually the same data is contained in the shape of the beam, for the total light power remains constant, and therefore a constant shape implies a constant maximum amplitude.

It is seen from these data that the shape of the deflected beam was quite accurately retained during deflection, although some minor distortion was generated by the shear-plate deflector. However, for the intended communication and tracking types of applications, the observed distortion is not serious. A practical measure of this distortion is the change in half-intensity spot diameter. For Model EOR2-2 the spot diameter varied from a minimum of 0.085 in. to a maximum of 0.095 in., or about 10 percent of the minimum value. For Model SPM-1, the diameter varied from 0.093 in. to 0.130 in., or 21 percent.

Figure 22 shows plots of deflection angle versus applied voltage for the same two deflector models. Solid lines show the actual data; dashed lines are zero-field straight-line asymptotes. The deflection angles were determined by measuring the motion of the "center of the spot," defined for these measurements to be the point midway between the half-intensity points. For all of these structures the deflection sensitivity increased with increasing voltage. The gains in sensitivity were quite significant, amounting to 7.2 percent at maximum fields in the EOR2-2 structure and 15.3 percent at maximum fields in the SPM-1 structure. It is quite apparent that for structures intended to provide maximum deflection of about 100 spot diameters, means must be devised for correcting this nonlinearity.

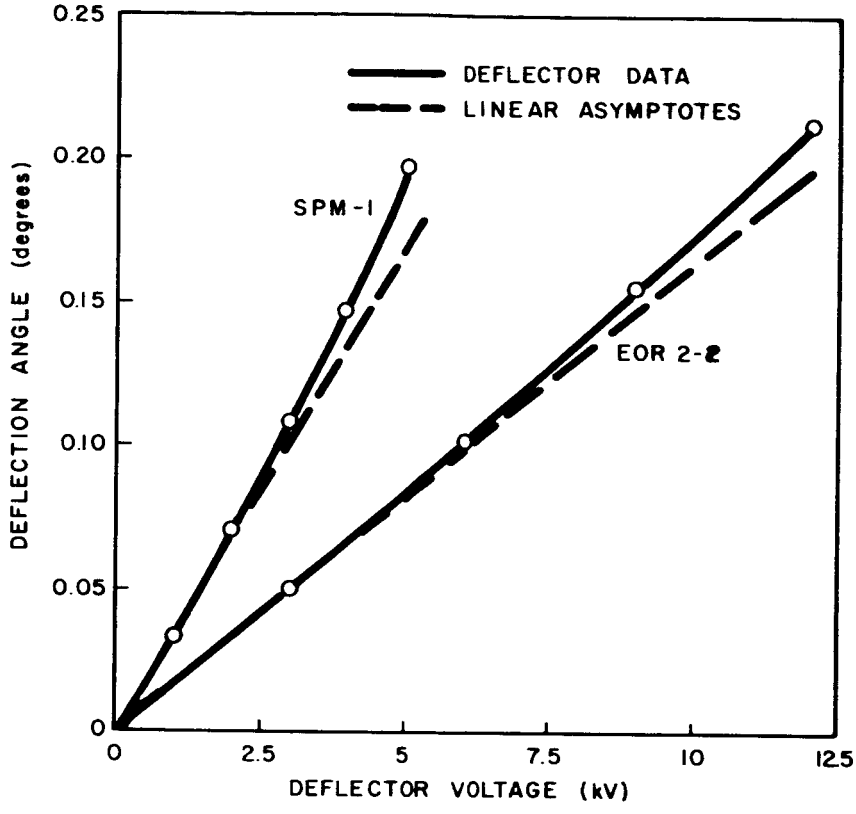

Fig. 22. Deflection control characteristics of refractor and reflector models.

5. SUMMARY AND CONCLUSIONS

This program was an investigation of electro-optic and piezoelectric methods for precision deflection of laser beams. The structures under investigation were all devices with inherent capabilities for extremely rapid deflection, exceeding the scan rate capabilities of mechanical devices, such as rotating mirrors. High-speed operation, however, was not an objective of this program.

It was determined that electro-optic refractors and shear-plate mirror reflectors could be designed to achieve deflection angles of about a degree for light beams with a minimum half-intensity beam angle of about 0.01 degree. The device embodiments have the inherent capabilities for achieving deflection rates in excess of 10 kc/s, and they can be made to have relatively low light loss in spite of the use of very large numbers of interfaces or mirrors. It was found that both the refractors and the reflectors required relatively large amounts of electrostatic energy to achieve maximum deflection, and the amount of energy is about the same for the two devices. However, the refractor can be made to operate with much lower deflection signal voltages. The large energy requirements make it impractical to use these devices with wideband deflection signals extending into the tens of kilocycles. However, the power required for structures using narrow-band deflection signals can be reasonably low even at very high frequencies, extending up to about 100 kc/s. Therefore, it is recommended that rapid scanning of a two-dimensional field can be accomplished using saw-tooth modulated quadrature sinusoidal signals on tandem horizontal and vertical deflectors to trace out a spiral scan.

Precision deflection with these devices appears to be feasible but difficult. The temperature of the active elements (electro-optic crystals or piezoelectric ceramics) must be maintained constant to within a fraction of a

degree, and means must be found to compensate or correct for nonlinear deflection experienced at high fields. Piezoelectric ceramics may pose special difficulties because these materials have characteristics which change slowly with the age of the material as the result of spontaneous depolarization. Furthermore, they are subject to partial depolarization when the applied voltage exceeds a certain threshold.

APPENDIX A

DERIVATION OF FORMULAS FOR VARIABLE REFRACTORS

A1. REFRACTORS OF THE FIRST KIND

Figure A1 shows what happens to light passed through the mth lower prism of a variable refractor of the first kind. The cross section of this prism is an isosceles triangle with base angle α. The beam enters at an angle φ_{m-1}, is refracted at the left and right surfaces, and emerges at an angle φ_m. The complements of the angles of incidence and refraction at the left surface are i_1' and r_1' and at the right surface are i_2' and r_2', where

$$i_1' = \alpha - \varphi_{m-1} , \qquad A(1)$$

$$i_2' = 2\alpha - r_1' , \qquad A(2)$$

$$\varphi_m = r_2' - \alpha . \qquad A(3)$$

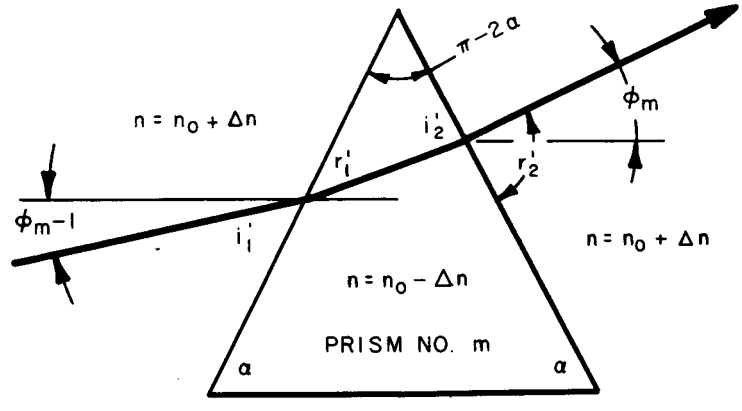

Fig. A1. Refraction of light beam by mth lower prism.

The complementary angles of incidence and refraction are related by Snell's equation, as follows:

$$(n_o+\Delta n)\cos i_1' = (n_o-\Delta n)\cos r_1' \qquad A(4)$$

$$(n_o-\Delta n)\cos i_2' = (n_o+\Delta n)\cos r_2' \qquad A(5)$$

In general Δn will be a very small number. Therefore, we can express φ_m as the first two terms of a power series in Δn. It is readily shown that this ezpression is

$$\varphi_m = \varphi_{m-1} + \frac{4\Delta n}{n_o} \frac{\sin 2\alpha}{\cos 2\varphi_{m-1} - \cos 2\alpha}. \qquad A(6)$$

The change in φ in passing through the mth lower prism will then be the small quantity

$$\Delta\varphi = \varphi_m - \varphi_{m-1} = \frac{4\Delta n}{no} \frac{\sin 2\alpha}{\cos 2\varphi_{m-1} - \cos 2\alpha} \qquad A(7)$$

We can consider the total deflection angle φ to be a continuous function of the quantity

$$u = \frac{4m\Delta n}{n_o}. \qquad A(8)$$

The rate of change of u with respect o φ can be approximated by $\Delta\mu/\Delta\varphi$, where

$$\Delta u = \frac{4\Delta n}{n_o}, \qquad A(9)$$

this being the change in u corresponding to passage through the mth prism. Therefore, we have

$$\frac{du}{d\varphi} = \frac{\cos 2\varphi - \cos 2\alpha}{\sin 2\alpha}. \qquad A(10)$$

Integration of this equation, subject to the boundary condition u = 0 at $\varphi = 0$, yields

$$u = \frac{\frac{1}{2}\sin 2\varphi - \varphi\cos 2\alpha}{\sin 2\alpha}. \qquad A(11)$$

It can be shown that for very small values of φ this reduces to the linear equation

$$\varphi = \frac{4m\Delta n}{n_o}\cot\alpha. \qquad \text{(small } \varphi\text{)} \qquad A(12)$$

For a structure with M lower prisms, having a combined base length of L and triangle height H, as shown in Fig. 1, we obtain

$$\cot \alpha = \frac{L}{2MH} . \qquad A(13)$$

Therefore, the total deflection through the M lower prisms can be expressed as

$$\varphi_M = \frac{2\Delta n}{n_o} \frac{L}{H} . \qquad \text{(small } \varphi\text{)} \qquad A(14)$$

The beam experiences one more refraction before leaving the structure, namely the refraction in passing out of the half-size upper prism into the air. We can ignore the effect of Δn in this refraction. Letting Φ denote the angle of the emerging beam, as shown in Fig. A2, we have

$$\Phi = \sin^{-1}(n_o \sin \varphi_M) \cong n_o \varphi_m \qquad A(15)$$

Therefore, for small values of φ_M and Φ, the output beam angle is

$$\Phi = 2\Delta nL/H. \qquad \text{(small } \Phi\text{)} \qquad A(16)$$

This same result can be obtained much more simply in another way. For small values of Δn, each ray entering horizontally will pass through the deflector structure in a nearly horizontal line. The total phase shift

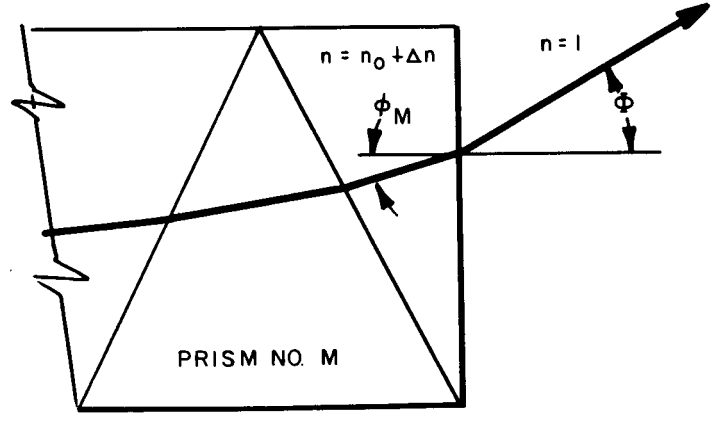

Fig. A2. Refraction at exit prism.

experienced by a ray of light traversing a certain path is proportional to the integral of n along that path. It is apparent from Fig. A3 that the integral of n along a horizontal path through the structure will vary linearly with the distance x measured perpendicularly to the bases of the prism. The phase of the light at C relative to the phase front $\overline{AB}$ of the input light will be

$$\text{phase at C} = \frac{2\pi}{\lambda_o} (n_o+\Delta n)L \qquad A(17)$$

and the phase at D will be

$$\text{phase at D} = \frac{2\pi}{\lambda_o} (n_o-\Delta n)L, \qquad A(18)$$

where λ_o is the free-space wavelength. The phase difference between C and D will be the difference,

$$\Delta\theta = \frac{4\pi}{\lambda_o} \Delta nL. \qquad A(19)$$

Line $\overline{CE}$ is a phase plane for the emerging refracted beam. Therefore, the phase of the light at E differs from the phase of the light at D by this amount. This phase shift corresponds to propagation through the distance d in air, for which the phase shift is $2\pi d/\lambda_o$. Setting this equal to the phase difference given above, we obtain

$$d = 2L\Delta n. \qquad A(20)$$

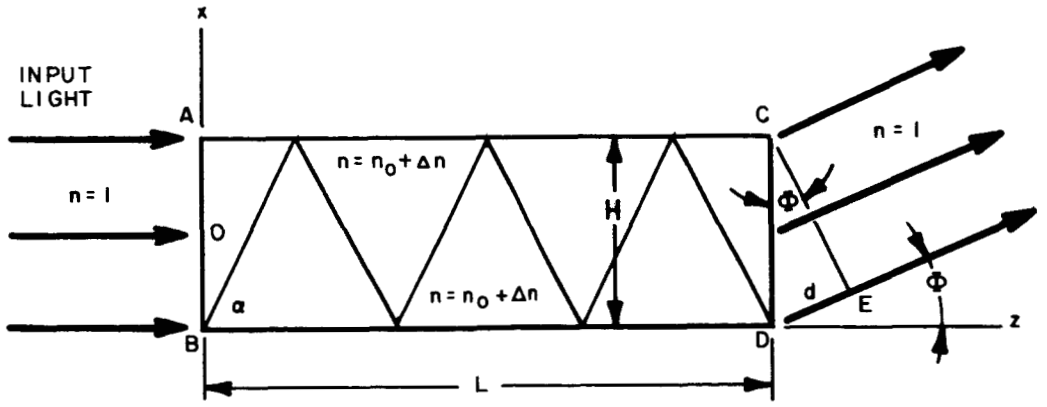

Fig. A3. Phase shift analysis of variable refractor.

From the figure it can be seen that

$$\Phi \cong \sin \Phi = d/H. \qquad A(21)$$

This leads to the same approximate formula for Φ obtained earlier, namely

$$\Phi = 2\Delta nL/H. \qquad A(22)$$

A2. REFRACTORS OF THE SECOND KIND

Figure A4 shows what happens to light passing through a variable refractor of the second kind. Let us assume that the material is actuated symmetrically about the center line x = 0, along which the index of refraction is n_o. The maximum change in refractive index will be called Δn, so that the index is $n_o - \Delta_n$ at $x - \frac{1}{2}H$ and $n_o + \Delta n$ at $x = +\frac{1}{2}H$. For small changes in the refractive index and short enough path lengths, the light will travel through the structure in nearly horizontal lines. Rays leaving A and B are initially in phase with each other, but as they travel along the edges $\overline{AC}$ and $\overline{BD}$, they are shifted in phase by amounts proportional to the index of refraction and the distance traveled in the z direction. The phase difference between the light at C and D will be

$$\Delta\theta = 4\pi L\Delta n/\lambda_o. \qquad A(23)$$

Line $\overline{CE}$ in Fig. A4 is a phase plane for the emerging refracted beam. Therefore, the phase of the light at E differs from the phase of the light at D by this same amount $\Delta\theta$. This phase shift corresponds to propatation through the distance d in air, for which the phase shift is $2\pi d/\lambda_o$. Setting this equal to $\Delta\theta$, we obtain

$$d = 2L\Delta n. \qquad A(24)$$

From Fig. A4,

$$\Phi \cong \sin \Phi = d/H. \qquad A(25)$$

This leads to the same approximate formula for Φ obtained above for the refractor of the first kind, namely

$$\Phi = 2\Delta nL/H. \qquad A(26)$$

The only difference is that Δn has acquired a new meaning. In both kinds of refractor, however, $2\Delta n$ is the difference in refractive index at the two edges of a rectangular prism of variable refraction material (a composite of many triangular prisms of homogeneous material in the device of the first kind, and a single inhomogeneous prism in the device of the second kind).

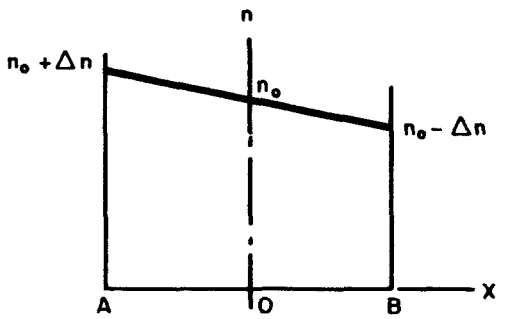

(a) Variation of n with X

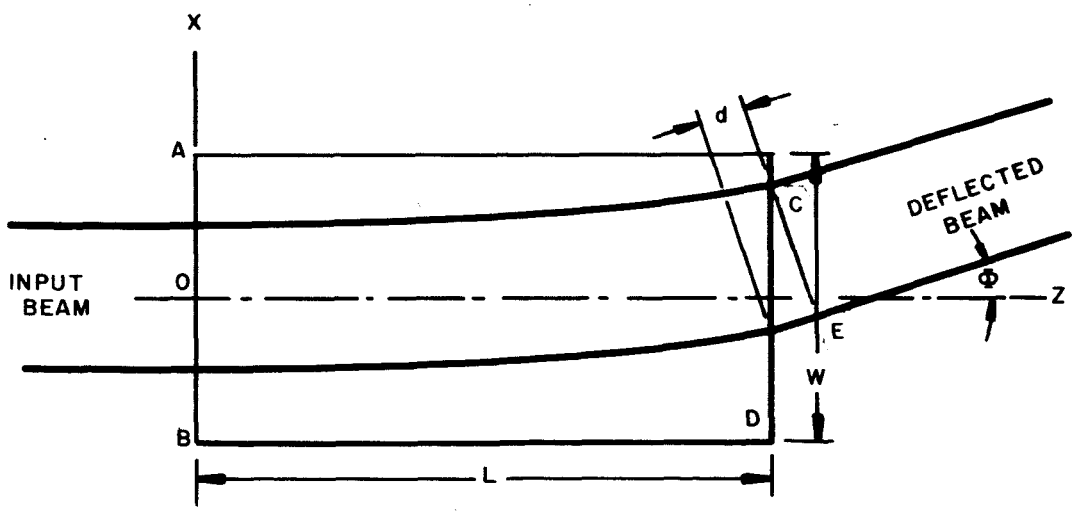

(b) Passage of light through structure

Fig. A4. Variable refractor of the second kind.

APPENDIX B

Derivation of Formula for Shape of Quadrupole Electrodes

To arrive at a closed-form solution for the shape of the quadrupole electrodes, we assume that the electro-optic crystal extends indefinitely far in the $\pm x$ directions, but is of finite thickness in the -y direction, the top surface being at $y = 0$. The formula to be derived is for the top pair of electrodes, which are in the first two quadrants of the x-y plane. The space between the top surface of the crystal ($y = 0$) and the top electrodes is filled with a uniform isotropic dielectric material of dielectric constant K_2. The crystal itself is uniform but anisotropic, having dielectric constant K_{y1} for field components in the y direction and K_{x1} for field components in the x direction. Using subscripts 1 and 2 to denote the crystal and the filler dielectric, respectively, one readily obtains the following formula for Laplace's equation for the anisotropic crystal:

$$K_{y1} \frac{\partial^2 V_1}{\partial x^2} + K_{y2} \frac{\partial^2 V_1}{\partial y^2} = 0. \qquad B(1)$$

The desired condition in the crystal is to have

$$\frac{\partial V_1}{\partial y} = K_1 x, \qquad B(2)$$

i.e., a y-directed field component proportional to x. Integration of Eq. B(2) yields the following generalized form for V_1:

$$V_1 = K_1 x y + f(x), \qquad B(3)$$

where f(x) is an arbitrary function such that V_1 satisfies Eq. B(1). Substitution of Eq. B(3) into Eq. B(1) reveals that

$$f''(x) = 0, \qquad B(4)$$

from which one obtains, by integration,

$$f(x) = Ax + B, \qquad B(5)$$

where A and B are constants of integration. The potential in the crystal is then

$$V_1 = K_1xy + Ax + B. \qquad B(6)$$

There is no loss in generality by making B = 0, since this affects only the reference potential. The axes x = 0 and y = -b/2, where b is the thickness of the crystal, are both axes of odd symmetry. Therefore, the potential should be an odd function of both x and y + b/2. This fixes the value of A to be

$$A = k_1 b/2, \qquad B(7)$$

and the potential in the crystal becomes

$$V_1 = k_1 x (y + b/2). \qquad B(8)$$

The boundary conditions at the top surface of the crystal (y = 0) are that the tangential component of the electric field is continuous and the normal component of the electric flux density is continuous. It is found that these conditions can be satisfied if the potential in the filler dielectric is of the following form:

$$V_2 = k_2 x (y + y_o), \qquad B(9)$$

where k_2 and y_o are constants. The boundary conditions can be expressed as

$$\frac{\partial V_1}{\partial x} = \frac{\partial V_2}{\partial x} \qquad B(10)$$

and

$$K_{y1} \frac{\partial V_1}{\partial y} = K_2 \frac{\partial V_2}{\partial y}. \qquad B(11)$$

Substitution of Eqs. B(8) and B(9) into Eqs. B(10) and B(11) yields the following values for the constants k_2 and y_o:

$$k_2 = k_1 K_{y_1}/K_2 , \qquad B(12)$$

$$y_o = b K_2/(2K_{y_1}). \qquad B(13)$$

It is convenient to have a formula for the shape of an equipotential curve in the region above the crystal, given a single point (X_1, Y_1) on that equipotential. For this point, the potential is

$$V_2(X_1, Y_1) = k_2 X_1 (Y_1 + y_o). \qquad B(14)$$

Setting this equal to V_2 in Eq. B(9), one obtains the following expression for the equipotential contour:

$$y = -y_o + (X_1/x)(Y_1 + y_o), \qquad B(15)$$

where y_o is given by Eq. B(13).

APPENDIX C

Scanning Photometer for Deflector Performance Tests

The function of this apparatus is to produce an oscilloscope display showing deflected laser beam intensity for eighteen adjacent positions on a line across the laser beam. Sampling of light intensity along this line is accomplished by passing the laser beam through a vertical slit in a rotating light chopper disc, and then through a horizontal slit in a stationary plate. The slit in the disc is in the form of a single-turn stepped spiral of eighteen steps. The disc and slit function as a small square aperture which jumps along a horizontal line, assuming eighteen fixed positions in sequence during one revolution of the disc. The light passing through this aperture is detected with a multiplier phototube, and the intensity is indicated by vertical deflection of an oscilloscope trace. The horizontal deflection frequency of the oscilloscope is made equal to the rotational frequency of the chopper disc, and the trace is initiated when the aperture is in the first of its eighteen positions. This is accomplished through the use of synchronizing signals derived photoelectrically from the disc. Additional synchronizing signals from the disc are used to trigger a bistable multivibrator which generates a square-wave signal voltage for application to the deflector under test. The frequency of this square wave is eighteen times the rotational frequency of the disc, and each cycle of the square wave starts when the aperture jumps from one position to the next.

This arrangement provides a display of eighteen full cycles of light intensity vs time as viewed from eighteen successive positions on a line across the beam. A stroboscopic display is obtained by unblanking the oscilloscope trace for ten microseconds at a selected interval after the start of each cycle of operation of the deflector,

thereby generating a display consisting of eighteen dots. The vertical positions of the dots are measures of the intensity of the light in the eighteen aperture positions at a selected time in the cycle of operation of the deflector. This time is determined by a time-delay generator used to generate the unblanking pulses from the multivibrator triggering pulses. The horizontal spacing between dots corresponds to the horizontal distance between the centers of adjacent aperture positions of the scanning disc.